Tomato pollen tube integrity is critical for pollen function at high temperature and is controlled by RALF signaling.

Rasha Althiab Almasaud**[1], Sorel V. Yimga Ouonkap**[1], Jared Ingram[1], Yahir Oseguera[1], Mohamed Alkassem Alosman[1], Cassandra Travis[1], Atticus Henry[1], Michelle Medina[1], Nathalie Oulhen[1], Gary Wessel[1], Alison DeLong[1], James Pease[2], Nick DaSilva[1], Mark A. Johnson[1]*

Department of Molecular Biology, Cell Biology, and Biochemistry; Brown University; 60 Olive Street, Providence, RI 02912, USA

Department of Evolution, Ecology and Organismal Biology; The Ohio State University; Aronoff Laboratory, 318 W. 12th Ave, Columbus, OH 43210, USA

** co-first authors, contributing equally
*corresponding

Corresponding authors:
M.A. Johnson (Lead Contact): mark_johnson_1@brown.edu

Abbreviations: HT, high temperature; Hz, Heinz; Mk, Malintka; Ng, Nagcarlang; Tm, Tamaulipas; RALF, Rapid Alkalinization Factor

Key words: crop productivity, heat resilience, thermotolerance, signal transduction, pollen tube integrity, RALF signaling

Acknowledgements:
This project was funded by grants from the US NSF (IOS-1939255) and the USDA/NIFA (2020-67013-30907). We thank Sherry Warner and Nick Vasquez (Brown University) for expertise in growing and maintaining tomato plants.

Author Contributions:
R.A.A., S.V.Y.O., J.I., Y.O., M.A.A., C.T., A.H., N.O., G.W., A.D. J.P., M.M., N.D., and M.A.J. conducted the experiments and developed the methods. R.A.A., S.V.Y.O., and M.A.J. analyzed the data. R.A.A., S.V.Y.O., and M.A.J. designed the experiments. R.A.A., S.V.Y.O., and M.A.J. wrote the manuscript.

Abstract

Reproductive success at high temperature (HT) depends on the ability of pollen to germinate a pollen tube that delivers sperm for double fertilization. We recently found that tomato cultivars capable of setting fruit at HT produce pollen tubes that continue to grow under heat stress. Our goal is to define the molecular basis of reproductive thermotolerance—the capacity to sustain cellular function at elevated temperature. Using quantitative live imaging, transcriptomic and proteomic profiling, and genetic analysis, we identified mechanisms distinguishing thermotolerant from thermosensitive tomato cultivars. HT accelerates pollen activation by increasing cell rupture in thermosensitive Heinz, whereas thermotolerant Tamaulipas and Nagcarlang maintain pollen tube integrity and elongation. Germination triggers broad transcriptional reprogramming, but corresponding proteomic changes are modest. We identify four pollen-expressed RALF peptides and show that RALF1, RALF3, and RALF4 repress germination at control temperature but signaling is antagonized by HT. Loss of *SlRALF1* enhances pollen tube integrity at HT in Heinz but delays successful germination in Tamaulipas, revealing cultivar-specific tuning of individual RALF function. HT and RALF signaling jointly modulate pectin organization at the tube tip, linking cell wall mechanics to reproductive resilience and establishing a mechanistic framework for generating heat-resilient crop plants.

Introduction

Erratic growing-season temperatures cause yield loss in crops[1], a problem expected to worsen as global food demand rises[2,3,4]. Many staple crops (wheat, rice, corn, fruits) depend on fertilization, yet this process occurs within a narrow thermal window[5–13]. Fertilization requires rapid (~1–12 h), long (~1000x initial diameter), highly polarized, and temperature-sensitive[14] pollen tube (PT) growth from stigma to ovules within an ovary[15]. Pollen grains, developed in anthers, germinate on the stigma, extend tubes guided through floral tissue[16,17], and rupture inside ovules to release two sperm for double fertilization[18], producing embryo and endosperm, the core of seeds. Because seed and fruit production depend on pollen performance—the ability to germinate, elongate rapidly, and avoid premature rupture—understanding the molecular basis of thermotolerant pollen performance is critical for improving crop resilience.

We recently found that heat stress applied only during the pollen tube growth phase is sufficient to limit tomato fruit and seed production[19]. We also showed that thermotolerant cultivars, which maintain fruit and seed set at high temperature (HT), have pollen tubes that grow better under HT (in the pistil and in vitro) than the Heinz reference cultivar[19]. However, these studies did not examine the early dynamics of pollen germination, tube extension, or the maintenance of pollen tube integrity—critical components of pollen performance.

Pollen tube integrity[20] is the ability of the PT to continue extending at its tip without bursting until it reaches an ovule and is essential for fertilization. Integrity is controlled by an autocrine signaling pathway in which rapid alkalinization factor (RALF) proteins[21–24] secreted by the PT are perceived on the plasma membrane by *Catharanthus roseus* RLK1-like receptors (e.g. ANXUR, ANX[20] and Buddha's Paper Seal, BUPS[23,25,26]) in concert with LORELEI-like glycosylphosphatidylinositol (GPI)-anchored proteins (LLG) co-receptors[25]. RALFs also directly modulate the cell wall through interactions with leucine-rich repeat extensin proteins (LRXs[24,27–29]). These signaling pathways have predominantly been studied in Arabidopsis, but RALFs were recently shown to control PT integrity in Maize[30]. Here, we test whether maintaining

integrity is a critical component of reproductive thermotolerance and whether RALFs contribute to pollen thermotolerance using tomato as a model.

Results

Pollen tube integrity distinguishes thermotolerant from thermosensitive pollen tube growth. Using live-imaging[31], we quantified pollen performance over two hours at 28° or 34° (Fig. 1, all temperatures reported in degrees Celsius). Previously, we examined heat stress on PTs after growth for 6 hours in vitro[19]; here, our goal was to analyze pollen function during the critical phases of germination and early elongation. Pollen from greenhouse-grown plants was incubated in growth media, and each grain in the field of view was classified in every frame (Fig. 1a–c). Hydrated grains (Fig. 1a,b, red square) were scored for "activation", either tube-producing (green square) or rupturing (blue square). Extending PTs were further classified as intact (green squares) or ruptured (cyan squares). PT tips were tracked across the time course to calculate extension rates (Suppl. Fig. 1). Dozens of grains were analyzed per replicate, with at least four replicates per temperature for each of six cultivars (Suppl. Figs. 1,2). Representative results from Heinz (reference), Tamaulipas (thermotolerant), and Nagcarlang (thermotolerant) illustrate the parameters distinguishing thermotolerant cultivars[19] (Fig. 1).

We found that germination occurred significantly earlier at 34°C (all temperatures, celsius) in all cultivars (Fig. 1c), indicating HT accelerates germination. Analysis of the fraction of activated (germinated or ruptured pollen) showed a small, but significant effect of HT, with time to 50% activation faster at 34° (solid lines) than at 28° (dotted lines, Fig. 1d). However, when examining successful germination, HT significantly affected only Heinz (Fig. 1e) and VF36 (Sup. Fig. 2c), both reaching a maximum of 65%. When we analyzed the fraction of ruptured pollen over time, we found that germination was reduced because over 30% of Heinz pollen ruptured at HT during the time course (Fig. 1f). Interestingly, this analysis also highlights that at both 28° and 34°, Tamaulipas and Nagarlang have very low pollen rupture rates that are

significantly lower than Heinz. These data suggest that thermotolerant cultivars have enhanced pollen performance at HT because they maintain PT integrity during activation and elongation.

Thermotolerant Nagcarlang modulates its pollen transcriptome and proteome in response to germination, but is relatively unaffected by HT. When we previously analyzed HT-induced gene expression in PTs grown for six hours in vitro[19], we found evidence of stress-response priming: thermotolerant Tamaulipas had higher basal levels of genes that were induced by HT in Heinz[19]. To test whether priming is also a feature of germination and early elongation, we also collected transcriptome and proteome data over two hours (Fig. 2a; blue stars, RNA-seq; green stars, proteome). Principal component analysis showed genotype is the primary driver of variance in global mRNA and protein expression (Fig. 1b; also observed in growing PTs[19]). Interestingly, transcriptome variance increased with time under HT (mature pollen vs. 120 min, Fig. 1b, Transcriptome), but proteome variance remained limited (Fig. 1b, Proteome).

Because avoiding rupture during germination is critical for thermotolerance (Fig. 1e), we compared differentially expressed genes (DEGs) and proteins (DEPs) between mature pollen and pollen that had germinated (30 minutes) at 28° and 34° (Fig. 2a). Thermotolerant Nagcarlang expressed ~3× more germination-associated DEGs and DEPs than Heinz or Tamaulipas (Fig. 2c). Heinz showed the largest proportion of DEGs/DEPs altered only at HT, while Nagcarlang had the fewest (pink, Fig. 2c), suggesting Nagcarlang broadly activates the genome during germination, with expression less perturbed by HT.

DEGs exceeded DEPs in all cultivars (Suppl. Fig. 6a) and overlap was low (≤15%; 83/568 in Nagcarlang, Suppl. Fig. 6b). While this disconnect could be partly due to higher RNA-seq sensitivity compared to proteomics, this finding may also suggest HT-induced RNA changes were not translated into protein changes, especially in thermosensitive Heinz. We used k-means clustering to define gene groups with shared patterns during germination at both temperatures (Suppl. Figs. 3,4; Tables 1,2) and, interestingly, stress response genes clustered

differently across cultivars. HSP101, the first HSP induced (30 min, 28° vs. 34°; Suppl. Fig. 5), marked stress responses in all cultivars, but clustered differently: in Heinz, with genes induced only at HT (Fig. 2d); in Nagcarlang and Tamaulipas, with genes responsive to germination at both temperatures. These results suggest successful germination in thermotolerant cultivars (Fig. 1e) is linked to stress gene induction under both permissive and HT conditions.

Analysis of the tomato pollen tube RALF signaling pathway. PT integrity during germination and elongation distinguishes thermotolerant from thermosensitive tomato cultivars (Fig. 1f). To test whether the PT integrity-controlling[23–25,30] RALF signaling pathway underlies thermotolerant pollen tube growth in tomato (Fig. 1f), we defined pollen expressed RALF peptides (Fig. 3a), and their potential receptors and co-receptors (Suppl. Fig. 7). The tomato genome encodes 10 RALF genes (SlRALF1–10, Suppl. Table 3) and we constructed a phylogeny with 37 Arabidopsis RALFs[32], to identify tomato candidates likely regulating PT integrity. SlRALFs 1-4 were abundantly expressed in mature pollen and PTs and SlRALFs 1, 3, and 4 form a small clade related to AtRALFs 4 and 19 (Fig. 3a) - the core ligands for the autocrine signaling pathway controlling PT integrity in Arabidopsis[23,24]. Notably, SlRALF3 was previously characterized (SlPRALF) and shown to control PT elongation[22].

SlRALF1, SlRALF3, and SlRALF4, like AtRALF4 and AtRALF19 (Fig. 3b), have sequences associated with RALF processing (a dibasic cleavage site for pro-peptide removal[21,22]), four conserved cysteine residues essential for proper folding[21,22], and a YY (double tyrosine) motif implicated in interaction with CrRLK1L receptor kinases[33]. In contrast, SlRALF2, the RALF with the highest mRNA abundance in tomato pollen (Fig. 3a), was in a clade by itself (Fig. 3a) and lacked these characteristic motifs (Fig. 3b), suggesting potential functional divergence. Structural modeling of mature peptides further underscores significant differences in SlRALF2's structure compared to the other peptides (Fig. 3c). Analysis of RALF genetic variation across thermotolerant and thermosensitive cultivars[19] identified a single amino acid variant in SlRALF3, where isoleucine (I^{94}) is replaced by valine (V) in the Tamaulipas cultivar.

This finding suggests that variation in RALF signaling across thermotolerant and thermosensitive cultivars is not likely due to variation in RALF sequence.

RNA-seq analysis of SlRALF1-4 levels during pollen germination and elongation (Fig. 2a) indicated that RALF peptides are not induced by heat stress, but did reveal significant decreases in transcript levels during pollen germination (mature pollen compared with 30 minutes of growth) for RALFs 1 and 4 at 28° in Nagcarlang and at 34° for Nagcarlang and Tamaulipas (Fig. 3e). Only RALF1 was detected in our proteome analysis and it was found to significantly decrease during germination (mature pollen compared with 30 minutes of growth) in Heinz at both temperatures (Suppl. Fig. 7c). These data indicate that RALF expression levels are not affected by growth at HT (34°), but that decreases in RALF expression could be important for the pollen germination process, which is in keeping with prior work showing that treatment with RALF peptides inhibits pollen tube[22,24,25,34] and root hair growth[35].

SlRALF treatment represses pollen activation and is opposed by HT. To test whether tomato pollen RALFs are active and whether activity is altered by HT and/or genetic background, we synthesized mature RALF peptides (1-4) and analyzed their effects on Heinz, Tamaulipas, and Nagcarlang pollen growth using our live-imaging system (Fig. 4). We used 1 μM RALF peptide because end-point analysis suggested this concentration would facilitate analysis of the kinetics of pollen germination, tube growth, and integrity; higher concentrations completely block pollen germination (Suppl. Fig. 8). SlRALF2, which had no activity in endpoint assays (Suppl. Fig. 8) and no RALF treatment (Fig. 4, Suppl. Fig. 9) were used as negative controls. Pollen performance was classified over two hours at 28° or 34° (Fig. 4a).

At 28°, SlRALF1 significantly delayed germination in all cultivars and SlRALF4 had a similar effect, but only on Heinz (Fig. 4b). These delays were significantly diminished at 34°, indicating that HT antagonizes RALF repression. SlRALF1 and SlRALF4 also delayed pollen activation (germinated + ruptured pollen), most strongly in Heinz and Tamaulipas, where activation never exceeded 60% (Fig. 4c). Nagcarlang pollen, by contrast, was more resistant to

RALFs: 50% activated within 40 minutes under SlRALF1 treatment, compared with 100 minutes for Heinz. At 34°, activation accelerated for treated samples in all cultivars, again showing that HT counteracts RALF repression.

Analysis of successful germination confirmed these trends: about half of SlRALF1- or SlRALF4-treated Heinz pollen failed to germinate in two hours, whereas Nagcarlang was significantly less repressed (Fig. 4d). Analysis of rupture kinetics revealed a two-phase response: during the first 35 minutes of germination, SlRALF4 suppressed rupture at both temperatures, but afterward rupture increased in treated samples (Fig. 4e, dotted lines with circles). In Heinz, SlRALF4 promoted rupture over time at both 28° and 34°, with 80% ruptured by 90 minutes at HT (Fig. 4e). SlRALF1 (solid lines with triangles) had little effect on rupture. In Nagcarlang, SlRALF4 promoted rupture at both temperatures, but effects did not synergize with HT as they did in Heinz. In thermotolerant Tamaulipas, rupture remained minimal, with only mild increases under RALF treatment (Fig. 4e).

Together, these results show that RALF1 and RALF4 repress germination and activation, effects that are antagonized by HT and modulated by cultivar, with Nagcarlang showing the greatest resistance. We propose that pollen tube RALF signaling is diminished by HT and that thermotolerant cultivars have optimized RALF signaling to maintain pollen tube integrity at HT.

Loss of SlRALF1 increases pollen tube integrity at HT in Heinz and delays germination in Tamaulipas. To test whether RALF signaling regulates thermotolerant pollen tube integrity, we generated *SlRALF1* loss-of-function mutants in Heinz (*ralf1-6*^{H}) and Tamaulipas (*ralf1-4*^{T}, Fig. 5a). We focused on SlRALF1 because it was detectable in our pollen proteomic analysis (Fig. 3e) and had peptide treatment effects distinct from those of SlRALFs 2-4 (Fig. 4). Prior studies in Arabidopsis[23,24] and Maize[30] suggested that loss/reduction of two pollen *RALFs* was necessary to reveal mutant phenotypes, so we tested whether quantitative live-imaging under HT in tomato could detect individual *RALF* functions.

Immunoblots with anti-RALF1 antibodies detected precursor and mature peptides in wild-type samples; both were absent in mutants (Fig. 5b). Immunolocalization showed SlRALF1 accumulates in the shank ant tip of wild-type pollen tubes, (Fig. 5c-d). LM19 antibodies, which are specific for unmethylated pectin[36], had a pattern similar to anti-SlRALF1. Quantification of anti-SLRALF1 signal indicated stronger shank localization than tip, with Heinz showing significantly increased shank signal at 34°, a shift not observed in Tamaulipas (Fig. 5d).

Live-imaging at 28° and 34° revealed cultivar- and temperature-specific mutant phenotypes (Fig. 5e–h). In Heinz, *ralf1-6*^{H} had little effect at 28° but enhanced pollen tube integrity at 34° - pollen rupture plateaued at ~10% by 30 minutes at 34° in *ralf1-6*^{H} (similar to Tamaulipas at 34°), but reached ~35% by 2 hours in wild-type (Fig. 5h). Successful germination at 34° also improved, reaching ~85% in *ralf1-6*^{H} mutants versus ~70% in wild-type (Fig. 5g). Thus, loss of SlRALF1 improves Heinz pollen tube integrity at HT.

In Tamaulipas, *ralf1-4*^{T} did not affect rupture (Fig. 5h) but significantly slowed activation (Fig. 5f) and germination (Fig. 5g) at both temperatures. Mutant pollen tubes also germinated significantly later than wild-type at both temperatures (Fig. 5e). Therefore, SlRALF1 reduces thermotolerance in Heinz by compromising pollen tube integrity under HT, but in thermotolerant Tamaulipas it modulates the kinetics of germination across a range of temperatures.

RALF-regulated pollen tube pectin distribution is altered by growth at HT. Having established that HT disrupts pollen performance by decreasing PT integrity (Fig. 1), that the effects of RALF treatments on pollen tube growth are counteracted by HT (Fig. 4), and that loss-of-function of RALF1 enhances thermotolerant pollen tube growth in Heinz (Fig. 5), we set out to address how HT and RALF signaling interact to control deposition of pectin, a key component of the pollen tube cell wall[37,38]. Methyl-esterified pectin is relatively fluid and enriched at the extending PT tip; whereas unmethylated pectin is relatively stiff and is enriched in the pollen tube shank[39]. Recently, it was shown that maize pollen tube RALFs are required for proper distribution of pectin to maintain pollen tube integrity[30]. We analyzed pectin distribution

using LM19 (unmethylated pectin-specific antibody[36]) and LM20 (methylated pectin-pectin antibody[36]) immunolocalization in pollen tubes grown in vitro for 2 hours at 28° or 34° (Fig. 6a).

First, we address how temperature affects the distribution of pectin in growing pollen tubes, comparing patterns in thermosensitive Heinz and thermotolerant Tamaulipas. LM19 fluorescence intensity increased significantly in the shank and tip (regions of interest, Fig. 6b, c, f, j) under HT in Heinz and Tamaulipas, indicating an increase of unmethylated (stiff) pectin across the pollen tube (Fig. 6; green, 28°; magenta, 34°). LM20 (methylated pectin) fluorescence is highest at the tip and levels of tip-focused LM20 signal were not significantly changed by HT (Fig. 6d, e, h, i) in Heinz or Tamaulipas. However, LM20 levels in the shank significantly increased with HT in thermotolerant Tamaulipas (Fig. 6). These data, along with similar analysis of Nagcarlang (Supplementary Figure 11), indicate that HT changes pectin distribution in the pollen tube wall and that these changes vary across thermotolerant and thermosensitive genotypes.

Next we address how RALFs affect pectin distribution. Treatment with 1μm SlRALF1 significantly increased the levels of LM20 in the tip of Heinz and Tamaulipas when grown at either 28° or 34° (Fig. 6a, b). This was not observed for either SlRALF4 (Fig. 6b) or SlRAFL2 (Supplementary Fig. 11), suggesting a specific function for SlRALF1. Moreover, in *ralf1-6*^{H} mutant pollen tubes, we found that LM20 levels significantly decreased in the tip relative to wild-type Heinz and that mutant levels could be restored by addition of exogenous SlRALF1 to mutants (Fig. 6c). Treatment with 1uM SlRALF1, SlRALF4 (Fig. 6a,b) or SlRALF2 (Suppl. Fig. 10) did not significantly alter the LM19 signal in the shank of PTs grown at 28° in any cultivar and loss-of-function of SlRALF1 (*ralf1-6*^{H} or *ralf1-4*^{T}) did not affect the LM19 signal in the shank, relative to wild-type controls at 28°. These data indicate that RALF1 is specifically required to regulate levels of methylated pectin at the pollen tube tip.

Discussion

Quantitative live imaging revealed that HT accelerated pollen activation but compromises pollen tube integrity in thermosensitive genotypes. In Heinz, HT increased pollen activation but decreased the fraction of pollen grains that successfully initiated tubes, resulting in higher rates of premature tube rupture (Fig. 1 d-f). In contrast, Tamaulipas maintained higher germination efficiency, with a larger fraction of pollen grains successfully initiating tubes, and had a significantly higher proportion of tubes that maintained pollen tube integrity under HT (Fig. 1f). HT also slowed tip growth in fast-growing Nagcarlang PTs, equalizing tip velocities across cultivars, while Tamaulipas tubes retained more consistent elongation (Suppl. Fig. 1). These observations suggest that the coordinated control of germination timing, tip velocity, and tube integrity appears to be critical for maintaining reproductive success under HT. Live imaging allowed analysis of pollen tube growth following synchronization of germination, providing a precise assessment of tip dynamics and pollen tube lifespan. HT has differential effects across genotypes; thermotolerant Tamaulipas and Nagcarlang maintain function by sustaining successful germination and pollen tube integrity, while thermosensitive Heinz shows reduced performance due to higher rates of failed germination and premature tube rupture (Fig. 7).

Thermotolerant and thermosensitive tomato cultivars exhibit distinct molecular responses to HT during pollen germination. In Nagcarlang, germination (comparing mature pollen, with pollen grown in vitro for 30’ at either 28° or 34°) triggered extensive transcriptional and translational reprogramming (Fig. 3c), suggesting a large germination gene regulatory network that is not affected by temperature. In contrast, Heinz had more than twice the significant transcriptional changes during germination at 34° than it did at 28°; yet these transcriptional changes did not confer effective stress tolerance (Fig. 1). Tamaulipas maintained a relatively stable transcriptome during germination at either temperature (fewer DEGs than Heinz or Nagcarlang, Fig. 3c). Notably, stress genes such as HSP101 clustered with

germination-responsive genes in Nagcarlang and Tamaulipas, but with heat-responsive genes in Heinz (Fig. 2d). These data are consistent with the proposal that optimal germination and pollen tube elongation require expression of genes that have been classically defined as stress-responsive[40,41] and add perspective to our recent finding that the transcriptome of pollen tubes grown in vitro for six hours was primed for stress responses in thermotolerant Tamaulipas[19]. Analysis of germination and early pollen tube growth suggests that stress-responsive genes are activated by germination in thermotolerant cultivars (Fig. 2d).

We identified a broad transcriptome response to pollen germination (Fig. 3c), but corresponding changes to the proteome were modest and the overlap between differentially expressed transcripts and proteins was low (Supp. Fig. 6). This disconnect could reflect the higher sensitivity of transcriptomic methods, but it will also be important to test the possibility that post-translational mechanisms, rather than transcriptional induction, are critical for modulating gene activity in the pollen grain to manage successful pollen germination and growth at HT.

RALF signaling controls thermotolerant pollen tube integrity. Analysis of the Arabidopsis model system established an autocrine signaling pathway that contols pollen tube integrity[20,23–25] and work in maize recently demonstrated that this pathway is broadly functionally conserved and important for crop plant fertility[30]. Our goal was to use quantitative analysis of pollen tube growth under HT (Fig. 1) to test the hypothesis that autocrine RALF signaling mediated thermotolerant pollen tube growth, which we recently described in tomato[19]. We used proteomic and transcriptomic analysis to define pollen tube expressed RALFs (Fig. 3) and receptors/co-receptors (Supplemental Fig. 7) and found that tomato pollen expresses fewer RALFs (n=4) than Arabidopsis (n=14,[42]), a single co-receptor (SlLLG2/3) compared with distinct LLG2 and LLG3 genes in Arabidopsis[25,43], and the same number of CrRLK1L receptor kinases (ANX1, ANX2, BUPS1, BUPS2[23,25]). Importantly, tomato SlRALF3 (Fig. 3a, previously named SlPRALF for Pollen RALF[22]) and Arabidopsis AtRALF4[34] had been shown to repress pollen tube

elongation and our observation that RALFs were down regulated during germination (transcriptome and proteome, Fig. 3d) prompted us to test the hypothesis that RALF signaling is central to the ability of thermotolerant cultivars to maintain pollen tube integrity under HT (Figs. 1, 7).

We found that SlRALF1 and SlRALF4 peptides inhibited germination across cultivars, but also noted that responses varied, suggesting genetic variation in pollen tube RALF signaling within Tomato (Fig. 4, Fig. 7a, b). Importantly, we found that HT counteracted RALF peptide inhibition of pollen activation and germination in Heinz and Tamaulipas. These data suggest that HT reduces the ability of RALF signaling to negatively regulate pollen activation and thus leads to hyperactivation and bursting of pollen tubes during germination and growth in thermosensitive Heinz (Fig. 1f, Fig. 7c).

To begin to test this idea we generated loss-of-function mutants in one of the four RALFs expressed in tomato pollen (SlRALF1, Fig. 3a) in both Heinz and Tamaulipas. In Heinz, loss of SlRALF1 enhanced pollen tube integrity at high temperature (Fig. 5h, fraction ruptured is significantly reduced in the mutant), effectively phenocopying thermotolerance. In contrast, loss of SlRALF1 in Tamaulipas, delayed germination (Fig. 5g). These data suggest RALF signaling is optimized for germination in thermotolerant Tamaulipas, but loss of SlRALF1 in Heinz may alter RALF signaling output such that pollen tube integrity is increased under high temperature. Analysis of additional RALF single mutants and higher-order mutants in both cultivars will be required to define how each pollen tube RALF contributes to thermotolerant pollen tube growth.

RALF signalling and HT interact to control pollen tube pectin distribution. In growing pollen tubes, dynamic distribution of methylated and unmethylated pectin defines a mechanical gradient required to maintain pollen tube integrity as the tip rapidly extends[37,44,45]. Our immunolabelling experiments demonstrate that HT alters this balance, increasing unmethylated (stiff) pectin across the tube and enhancing methylated (soft) pectin in the shank of thermotolerant Tamaulipas (Fig. 6, Fig. 7d). We also found that treatment with exogenous

RALF peptides has distinct effects on pectin distribution. Treatment with SlRALF1 promoted methylated pectin at the tip in Heinz and Tamaulipas (Fig. 6 e,j), while loss of function (*ralf1-6*^{H}) only reduced tip-localized methylated pectin in Heinz (Fig. 6 e, j). These differences in the response to exogenous peptide versus loss of function could be important for understanding why loss of ralf1 leads to enhanced thermotolerance in Heinz.

Thermotolerant signal transduction as a means to achieve reproductive resilience in crop plants. Our results suggest that thermotolerance can be achieved by altering the composition of RALF proteins secreted by the pollen tube (Fig. 5h), and the antagonism we observed between HT and RALF signaling raises important questions about how temperature alters signal transduction. One possibility is that HT reduces RALF signaling (Fig. 7c) by altering the interactions among signaling components. Under this model, thermotolerance could emerge by genetic variation in signaling components that enhance function at HT. We've observed modest and focused genetic variation among RALFs (Fig. 3b) and receptors (Supplementary Fig. 7d) in the small set of tomato cultivars we've analyzed and future work will be aimed at testing whether this variation is required for thermotolerant pollen tube integrity.

Our prior work established that HT applied only during the pollen tube growth phase is sufficient to reduce fruit and seed production in tomato[19]. Here, we've shown that the ability to maintain pollen tube integrity is the pollen performance parameter that best distinguishes thermotolerant from thermosensitive cultivars (Fig. 1, 7) and that RALF signaling controls thermotolerant pollen tube integrity (Figs. 4 and 5, 7). Thus, this work establishes a mechanistic framework for developing heat-resilient reproduction in flowering plants and provides an avenue to develop crop varieties that can maintain yield when heat waves occur during the pollination season.

Materials and Methods

Plant materials and growth conditions. Solanum lycopersicum (tomato) plants of the Heinz cultivar were grown under a 13-h-day/11-h-night cycle in the Brown University Research Greenhouse. Plants were propagated either from rooted cuttings of self-fertilized lines or from seeds. Seeds of Heinz 1706-BG (LA4345), Tamaulipas (LA1994), and Nagcarlang (LA2661) were obtained from the Tomato Genetics Resource Center, UC Davis . For seed-based propagation, tomato seedlings were germinated in potting soil under standard greenhouse conditions (16-h-day/8-h-night cycle, 25 °/18 ° day/night temperature) in a controlled growth chamber for two weeks before being transferred to two-gallon pots. Plants were fertilized with Israel Chemicals Limited Peters Professional 5-11-26 Hydroponic Special and adequately watered. Daily temperatures were weather-dependent, fluctuating between 21° and 28° during the day and 16.5° to 18° at night, but were relatively regulated to optimal growth conditions. To maximize flower production, fruits and stems were regularly trimmed.

Live imaging of PT performance in vitro. Less than 30 minutes prior to live imaging, pollen was collected from 4 to 5 flowers using a modified vibrating toothbrush, added to a pre-warmed pollen growth medium, place in a secondary contained filled with temperature ready water and placed under a microscope inside a temperature ready incubator for imaging for 125 minutes as explained in Ouonkap et. al. 2025[31]. Movie recordings were performed at 14 frames per second then reduced to 125 frames 1 minute apart from one another before quantification with TubeTracker[31] with default settings. All automated qualifications were manually checked to correct for mistakes made through automated steps. Once pollen in each frame was classified as hydrated (red), ruptured as a grain (blue), ruptured as a tube (cyan) and viable and going (green, Fig. 1a,[31]) and raw files containing the information about each grain were then integrated together in R to extract information about pollen tube activation, germination, tip elongation and pollen cell integrity over time. All raw files, videos, and analysis

scripts are available in supplementary data and TubeTracker is available on github at https://github.com/souonkap/TubeTracker.

RNA extraction and RNAseq analysis. Dry mature grains and PT RNA were extracted as follows: Pollen was collected from young flowers and grown in vitro according to the method described in Ouonkap et al. 2024[19]. The collected pollen was then transferred to 2 mL Eppendorf tubes by centrifugation and immediately flash frozen in liquid nitrogen. PT samples were ground using a TissueLyser II (Qiagen) for 1 min. RNA isolation was performed using the ReliaPrep™ RNA Tissue Miniprep System kit (Promega). Subsequently, the RNA samples were stored at -80° until processing. RNA-seq data were analyzed as described in Ouonkap et al. 2024[19]. All RNA-seq data are available on the Sequence Read Archive (SRA) at https://www.ncbi.nlm.nih.gov/sra under the accession number [PRJNA980666, PRJNA611819].

Protein extraction and analysis. For protein extraction, pollen tubes were collected and the media was removed by centrifugation at 13000xg for 15 minutes. The cells were then ground using a TissueLyser machine. Afterward, the cells were washed with PBS. Subsequently, 200 µL of protein extraction buffer (5% SDS, 50mM Tris HCl, and 8M Urea, pH 7.55) was added. The mixture was incubated on ice for 30 minutes. To remove cell debris, the lysate was clarified by centrifugation at 13,000 x g for 10 minutes at 4°. The supernatant containing soluble proteins was carefully transferred to a tube on ice for analysis. The protein concentration was measured with the Bradford assay (Bio-Rad). The lysate was stored at –80° until processing.

Sample preparation for proteomic analysis using S-Trap method Samples were reduced using Dithiothreitol (DTT, 10mM final concentration, Sigma Aldrich, 646563-10X.5ML) and incubated at 55° for 45 minutes with mixing. Following incubation, samples were alkylated using Iodoacetamide (IAM, 20mM final concentration, Thermo Scientific, A39271) and incubated at room temperature in the dark for 30 minutes. Following alkylation, samples were acidified using Phosphoric Acid (2.5% final concentration, Sigma Aldrich, 79617-250ML), and vortexed for 30

seconds. 900mL of ice-cold Binding Buffer (9 parts LC/MS Grade Methanol (ACROS Organics, 61513-0025):1 part 1M TEAB (100mM Final concentration)) was added to each sample before the entire sample was transferred to each S-Trap spin column and centrifuged for 30 seconds at 4000xg. Each sample was then washed once with 150mL of binding buffer. Following protein washing, 1 vial (20mg) of Trypsin (Promega, V5111) was reconstituted in 50mM Triethylammonium Bicarbonate (TEAB, Sigma Aldrich, T7408) and added to each micro spin column to yield a final concentration of 1mg of trypsin for 20mg of protein in 100mL. Samples were then moved to a humidified chamber in a 37° incubator and left overnight (18hrs). On Day 2, samples were left to cool to room temperature for 15 minutes before 40mL of 50mM TEAB was added and each sample was centrifuged for 1 minute at 4000xg. Peptides were eluted with 40mL of LC/MS grade Water (Honeywell, 39253-4X2.5L) and 0.1% Formic Acid (Fisher Scientific, A117-50), and centrifuged again for 1 minute at 4000xg. Finally, to completely elute hydrophobic peptides, 40mL of 50% LC/MS Grade Acetonitrile (Fisher, A955-4) was added to each sample and allowed to stand for 5 minutes before being centrifuged for 1 minute at 4000xg. Each sample was concentrated using a speed vacuum concentrator (Thermo Fisher Scientific) for approximately 90 minutes. With solvent removed, samples were reconstituted in 100mL of Solvent A (Water with 0.1% Formic Acid) and spiked with indexed retention time peptides (Biognosys, Ki-3002-1) in a 1:50 dilution to monitor HPLC performance.

LC-MS proteomic analysis. Samples were then injected onto a QExactive Orbitrap LC/MS system (Thermo Fisher Scientific) and separated over a 120-minute gradient consisting of solvent A (water + 0.1% Formic Acid), and solvent B (Acetonitrile and 0.1% Formic Acid) using a split-flow set-up on an Agilent 1200 series HPLC system. A 15cm long (75mm ID) capillary analytical column packed with XSelect CSH C18 2.5 mm resin (Waters) from the University of Arkansas for Medical Sciences (UAMS) IDeA National Resource for Quantitative Proteomics was used to separate digested peptides. The 120-minute gradient consisted of 95%

Solvent A for 1 minute, 70% solvent A for 94 minutes, 5% solvent A for 6 minutes and finally 100% solvent A for the remaining 20 minutes all at a flow rate of 0.240 ml/min. The mass spectrometer acquisition utilized a Full MS/ddMS2 (Top9) centroid experiment. Full MS parameters used a default charge state of 2, 1 microscan, resolution of 70,000, AGC target of 3e6, 200ms Maximum Injection time, in a scan range of 400-1800m/z. ddMS2 parameters were 1 microscan, resolution of 17,500, AGC target of 2e4, a max injection time of 200ms, a loop count of 9, Top 9 precursors, Isolation window of 2.5m/z, collision energy of 28, and a scan range of 200-2000 m/z. Data dependent settings consisted of a minimum AGC target of 2e2, 1e3 intensity threshold, unassigned charge exclusion, all charge states, preferred peptide match, isotope exclusion, 30 seconds of dynamic exclusion.

Label free quantitation and MaxQuant search parameters. Raw files were processed using MaxQuant (Ver 2.1.4) using 1% peptide and protein FDR search constraints, all values were default except for 20ppm first search tolerance and 7 ppm main search tolerance against Heinz Tomato protein fasta file (ITAG4.1). Variable modifications consisted of just oxidation (M) and protein N-terminal Acetylation. Carbamidomethylation was the sole static modification for the Trypsin/P search. Match between runs algorithm was unselected and intensity-based absolute quantification (iBAQ) was selected. The proteingroups.txt file output was further processed in MS Excel and Relative IBAQ was calculated as the intensity of each protein divided by the sum of all intensities for each given sample. The mass spectrometry proteomics data have been deposited to the ProteomeXchange Consortium via the PRIDE [46] partner repository with the dataset identifier **PXD053410**. DEqMS package was used to calculate differential protein expression (DEP) https://www.bioconductor.org/packages/devel/bioc/vignettes/DEqMS/inst/doc/DEqMS-package-vignette.html .

Alignment and phylogenetic analysis of RALF peptides, receptors, and co-receptors. Protein sequences of RALF peptides were obtained from the Sol Genomics

Network (ITAG4.1) for tomato and from the TAIR database (TAIR11) for Arabidopsis. Multiple sequence alignment (MSA) was performed using the MUSCLE method. The phylogenetic tree was constructed based on the neighbor-joining statistical method, with 100 bootstrap replicates. For the alignment of RALFs, predicted signal peptides and propeptides (if present) were removed, and only the predicted mature RALF sequences were used.

Ralf peptide design. All peptides (Sup. Table S5) used in this study were synthesized by Biomatik with purity >95%. They were diluted in ddH2O.

PT Immunolocalization. Immunolabeling was performed as previously described by [47]. Pollen grains were collected and allowed to germinate for 2 hours, after which PTs were collected, fixed in paraformaldehyde-based fixation solution, and stored at 4° until use. Fixed PTs were washed with PBS, incubated in a blocking solution, and then treated overnight at 4° with anti-LM19 or anti-LM20 antibodies for weakly or highly methylesterified HGs, respectively (Kerafast, https://www.kerafast.com). After washing, PTs were incubated with Alexa488-conjugated secondary antibodies, followed by additional washes. Control samples were treated with the secondary antibody only. Immunolabeled PTs were visualized using an inverted Nikon Ti2-E Widefield Fluorescence Microscope under identical imaging conditions, and fluorescence intensity was analyzed using ImageJ software.

Generation of *RALF1* CRISPR/Cas9 Mutants. To generate CRISPR/Cas9-induced mutations in the *RALF1* gene, we used the CRISPR-P web tool (http://crispr.hzau.edu.cn/CRISPR2/) to design two guide RNAs. The guides were carefully selected to target regions upstream of the mature peptide or motif-encoding sequences, ensuring disruption of *RALF1* function. The CRISPR/Cas9 construct was assembled using the GoldenBraid cloning strategy. The final plasmid was then sent to Dr. Thomas Clemente's laboratory at the University of Nebraska for Agrobacterium-mediated transformation. Seeds from Tamaulipas and Heinz cultivars were used for transformation to assess the effect of *RALF1* disruption in contrasting genetic backgrounds.

Western Blot Analysis. Proteins were separated by SDS-PAGE on 4–12% acrylamide gels and transferred onto 0.22-μm nitrocellulose membranes [48]. Running and transfer buffers were obtained from Invitrogen. Membranes were blocked and incubated overnight at 4° with rabbit polyclonal antibodies (Boster) against RALF1 (1:1000), and PEPC (1:3000) (ref) in 20 mM Tris-HCl (pH 7.4), 150 mM NaCl, 0.1% Tween-20, and 2% BSA. After washing, membranes were incubated for 1 h at room temperature with horseradish peroxidase–conjugated secondary antibodies. Protein expression was detected by chemiluminescence following the manufacturer's instructions (ECL, Pierce 32106) and imaged using the ChemiDoc™ MP Imaging System (Bio-Rad Laboratories, Hercules, CA, USA). Images were analyzed with Image Lab. Software (Version 2.3.0.07).

Figures

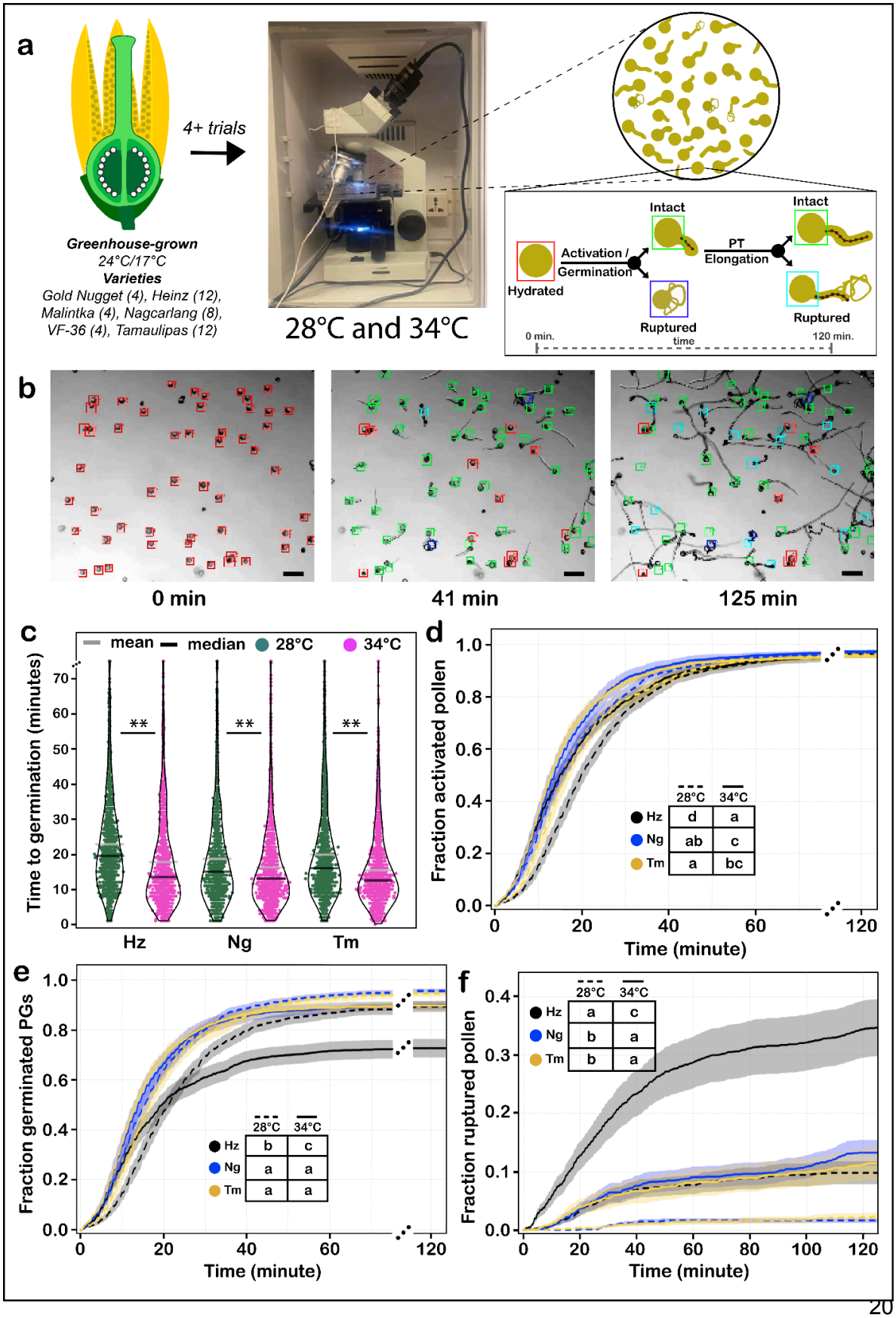
a
4+ trials
Greenhouse-grown
24°C/17°C
Varieties
Gold Nugget (4), Heinz (12),
Malintka (4), Nagcarlang (8),
VF-36 (4), Tamaulipas (12)
28°C and 34°C
Hydrated
Activation / Germination
Intact
Ruptured
PT Elongation
Intact
Ruptured
0 min.
time
120 min.
b
0 min
41 min
125 min
c
mean
median
28°C
34°C
Time to germination (minutes)
Hz
Ng
Tm
d
Fraction activated pollen
Time (minute)
28°C 34°C
Hz d a
Ng ab c
Tm a bc
e
Fraction germinated PGs
Time (minute)
28°C 34°C
Hz b c
Ng a a
Tm a a
f
Fraction ruptured pollen
Time (minute)
28°C 34°C
Hz a c
Ng b a
Tm b a

Figure 1: Live cell imaging of pollen growth reveals that high temperature promotes activation/germination and rupture, leading to decreased performance for thermosensitive Heinz. (a) Illustration of our approach to study the impact of temperature stress on pollen performance using live imaging. The numbers in parentheses (left) represent the number of trials per cultivar. Colored squares (right) represent pollen states tracked in each recording. **(b)** Representative images (Heinz) of the tracking results of germination and viability during germination and early elongation. The colored boxes indicate the state of each pollen as in (a). **(c)** Time to successful germination at indicated temperatures. Each dot represents a germinated pollen grain. Statistical analysis was performed using the Mann-Whitney-Wilcoxon U test using p.value thresholds of ns > 0.01 > * > 0.001 > **. **(d)** Fraction of activated pollen grains over time – grains that germinated a tube (green) or burst (blue or cyan). **(e)** Fraction of successfully germinated pollen grains over time (green). **(f)** Fraction of ruptured pollen grains and tubes over time (blue or cyan). For **d-f,** Statistical analysis was performed using survival analysis (methods) with a time cutoff of 125 minutes and pairwise p.values were bonferroni adjusted. Similar letters in tables represent no statistical significance between groups at a p.value < 0.01. Different letters in tables represent statistically significant differences at a p.value < 0.01 between groups.

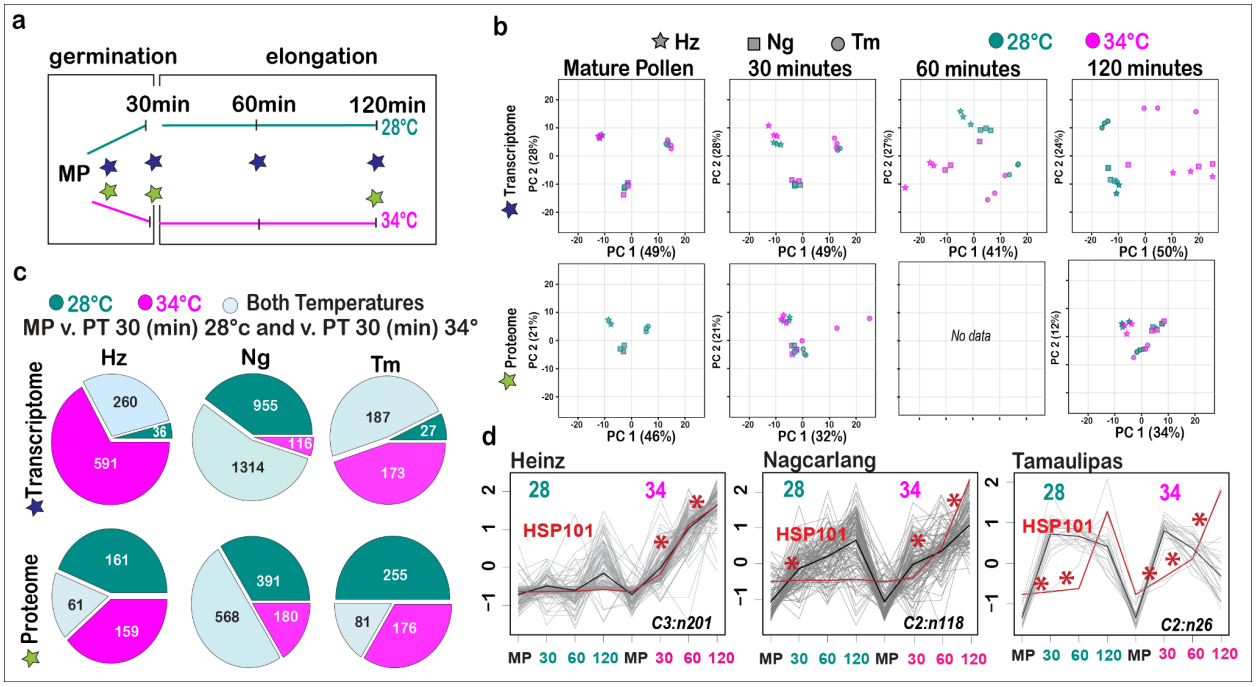

Figure 2: Germinating pollen of thermotolerant cultivars exhibit distinct transcriptomic and proteomic responses to HT. (a) Time points used for transcriptome (blue star) and proteomic (green star) analysis. **(b)** PCA was performed on transcriptomic data from mature pollen samples at 30, 60, and 120 min after germination, and on proteomic data at 30 and 120 min post-germination, across Heinz (Hz), Nagcarlang (Ng) and Tamaulipas (Tm) cultivars. Each point on the plot represents a sample, with its position determined by the first two principal components capturing the most significant variance in the data. **(c)** Pie chart presents the distribution of differentially expressed genes (DEGs) and proteins (DEPs) between mature pollen and pollen tubes at 30 min, at 28° and 34° across three cultivars. **(d)** The transcriptomic cluster (Suppl. Fig. 3) containing heat stress indicator, HSP101, for each cultivar. The cluster number and the number of genes in each cluster is provided. Red stars denote statistically significant differences in expression between time points.

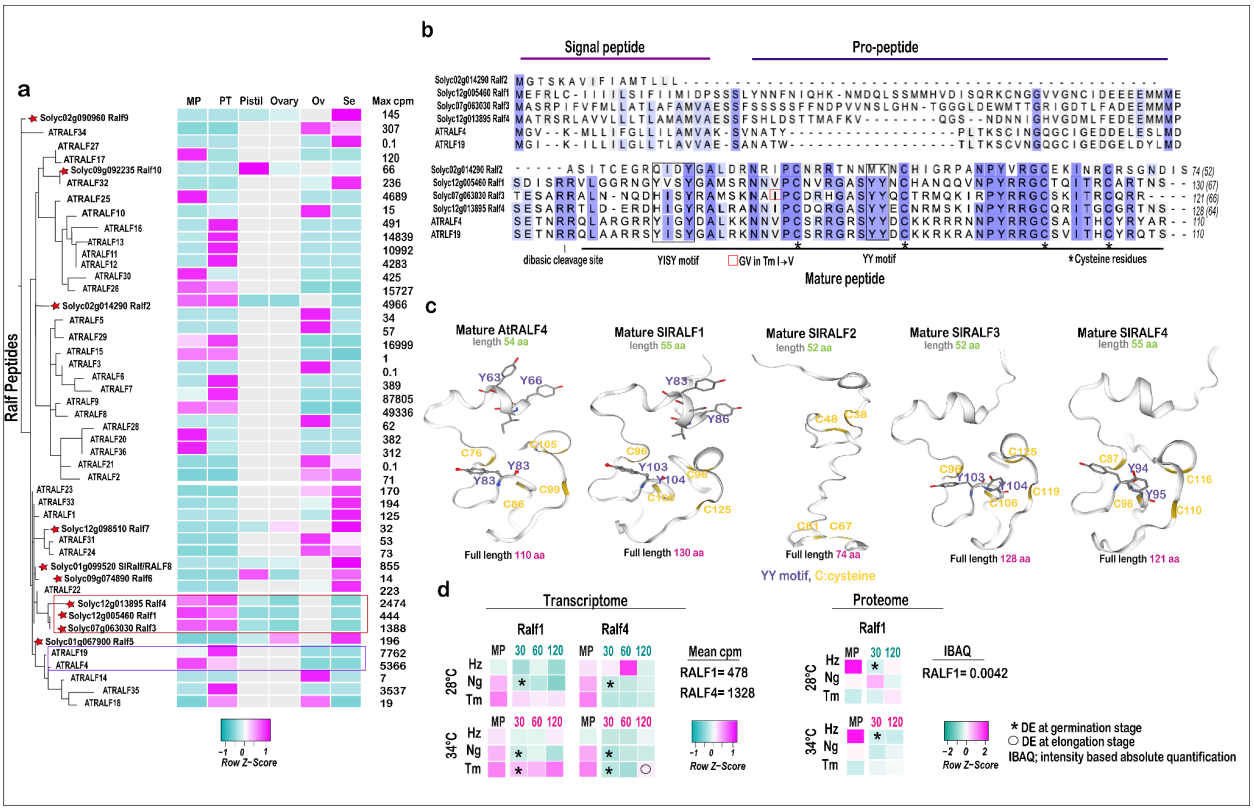

Figure 3: Tomato pollen expresses 4 RALFs. (a) Phylogenetic tree illustrating the evolutionary relationships between tomato peptides and Arabidopsis Ralfs peptides. Additionally, a heatmap shows the expression levels of these peptides in different tissues such as mature pollen "MP", pollen tube "PT", pistil, ovary, ovule "Ov" and seedling "Se". Max cpm represents the highest expression value observed across the different tissues. Gray boxes in the heatmap indicate tissues for which data are missing or not provided. **(b)** Peptide alignment comparing the most abundant RALF peptides found in tomato mature pollen with Arabidopsis pollen-expressed RALFs. The length of the predicted mature peptides is shown in parentheses following the total amino acid count. Alignments were visualized using the UniProt alignment tool (https://www.uniprot.org/align). **(c)** Structural models of the mature peptides of Arabidopsis RALF4 (AtRALF4) and tomato SlRALF1, SlRALF2, SlRALF3, and SlRALF4 highlight conserved

YISY and YY ring motifs essential for receptor binding, along with cysteine residues (C). The models were generated using SWISS-MODEL. **(d)** Heatmap representation showcasing the expression levels of RALF1 and RALF4 , at both transcriptomic and proteomic levels across various time points and cultivars, under control and heat stress conditions. The significance of expression changes is denoted by stars (*) at the germination stage and circles (o) at the tube elongation stage. Colored time point labels indicate cyan for control temperature (28°) and magenta for high temperature (34°).

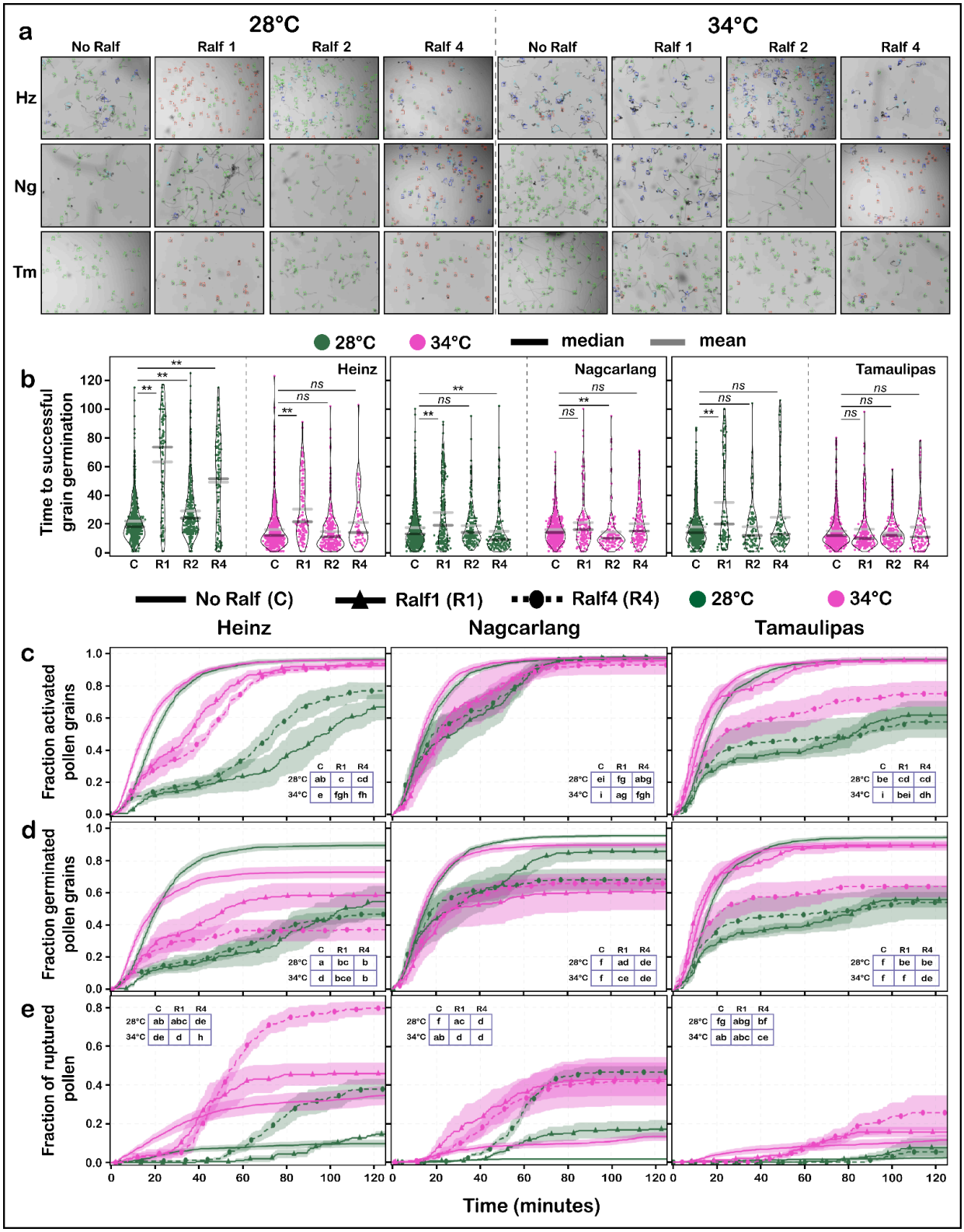

Figure 4: Effects of Ralfs and Temperature on pollen grain activation, germination, and cell rupture. (a) Representative images of pollen tube growth and data quantification after 60

minutes of growth. **(b)** Time to successful germination at indicated temperatures and in the presence of 1uM Ralf 1, Ralf 2, or Ralf 4. Each dot represents a germinated pollen grain. Statistical analysis was performed using the Mann-Whitney-Wilcoxon U test using p.value thresholds of ns > 0.01 > * > 0.001 > **. **(c)** Fraction of activated pollen grains over time – grains that exited the hydrated state (Figure 1a, red). **(d)** Fraction of successfully germinated pollen grains over time (Figure 1a, red to green). **(e)** Fraction of ruptured pollen grains and tubes over time (Figure 1a, blue + cyan). For c-e, Statistical analysis was performed using survival analysis (methods) with a time cutoff of 125 minutes and pairwise p.values were bonferroni adjusted. Similar letters in tables represent no statistical significance between groups at a p.value < 0.01. Different letters in tables represent statistically significant differences at a p.value < 0.01 between groups.

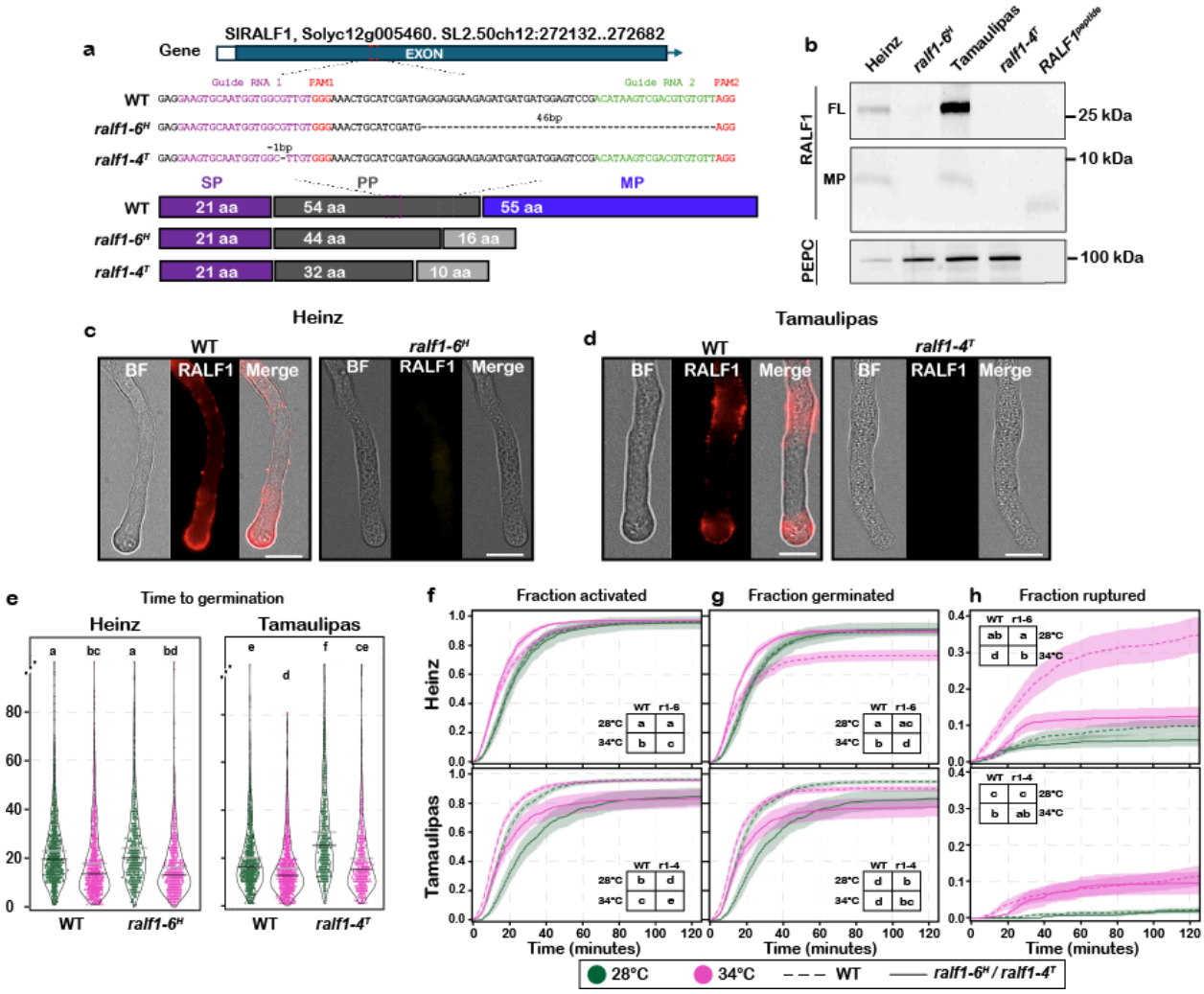

Figure 5. RALF1 localization and pectin deposition in tomato pollen tubes. (a) Schematic of CRISPR-Cas9 generated ralf1 mutants in Heinz (ralf1-6) and Tamaulipas (ralf1-4) showing deletion of the mature peptide coding sequence. **(b)** Western blot analysis was performed using anti-RALF1 antibodies on protein extracts from WT Heinz, WT Tamaulipas, ralf1 mutant lines, and the synthetic RALF1 peptide (Supplementary Figure 10). Phosphoenolpyruvate carboxylase (PEPC) was used as a loading control for the same samples. FL: full-length and MP: mature peptide. **(c, d)** Representative immunolocalization images of RALF1 at 90 minutes after pollen germination in Heinz and Tamaulipas, respectively. **(e)**, fraction of activated pollen **(f)**,

germinated pollen **(g)**, and ruptured pollen **(h)** over time. Statistical significance was determined using the Kruskal–Wallis test and Man-Withney-Wilcoxson (e) and survival analysis (f-h) and resulting pairwise p.values were Bonferroni adjusted. For each panel (e-h), similar letters indicate no statistical significance at $p < 0.01$ and different letters indicate statistical significance at $p < 0.01$.

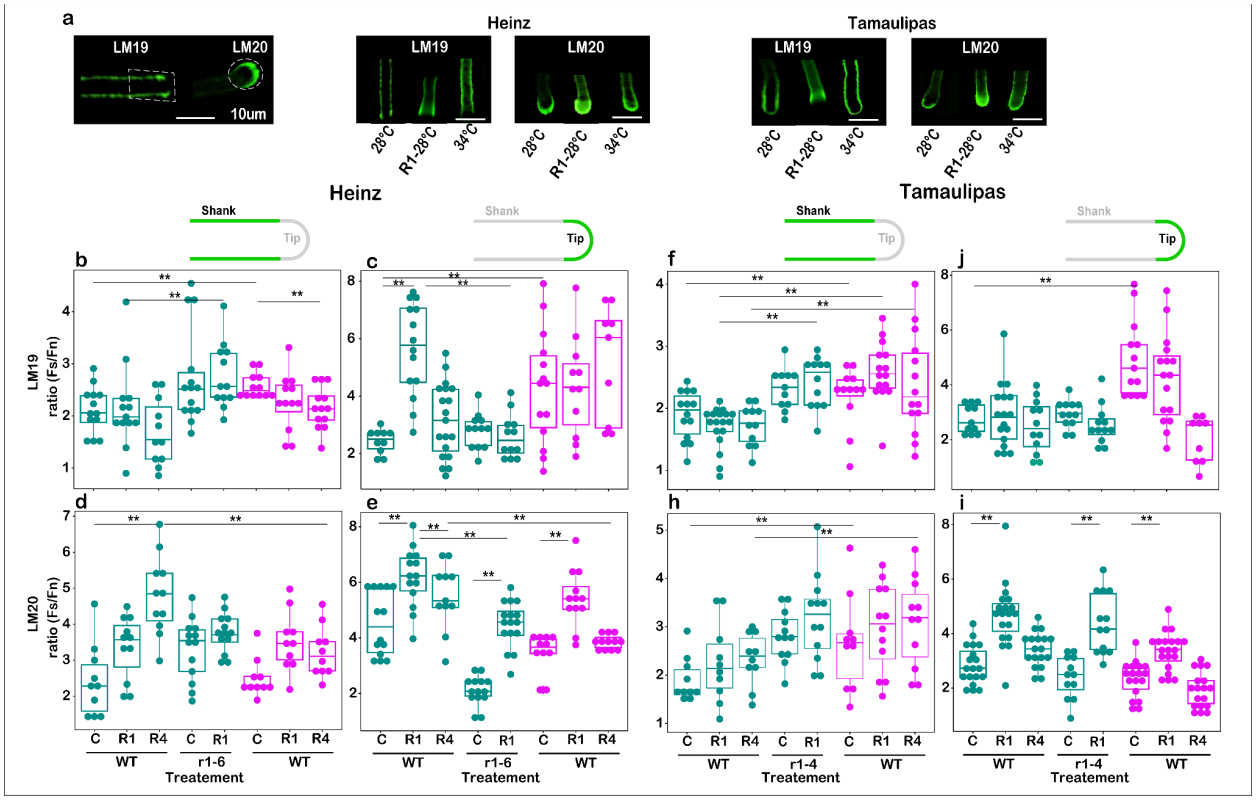

Figure 6: RALF signalling and temperature interact to control pectin localization in pollen tubes. (a) Representative images of LM19 and LM20 immunostaining, showing pectin distribution in the shank and tip regions of pollen tubes, respectively, across tomato cultivars. RALF1 (R1) treatment is used as a representative for staining patterns. Dashed lines indicate the regions of interest (ROI) measured for fluorescence intensity. **(b-i)** Quantification of fluorescence intensity for LM19 and LM20 staining in the shank and tip region under RALF1, RALF4 treatments across cultivars Heinz, Nagcarlang *(Supplementary Figure 11)*, and Taumalipas , and at 23° and 34°. Fluorescence intensity was normalized using the ratio of LM19 or LM20-stained fluorescence (Fs) to fluorescence of unstained controls (Fn). Statistical significance was determined using Dunn test and indicated as $p < 0.01$ (**), and ns (not significant).

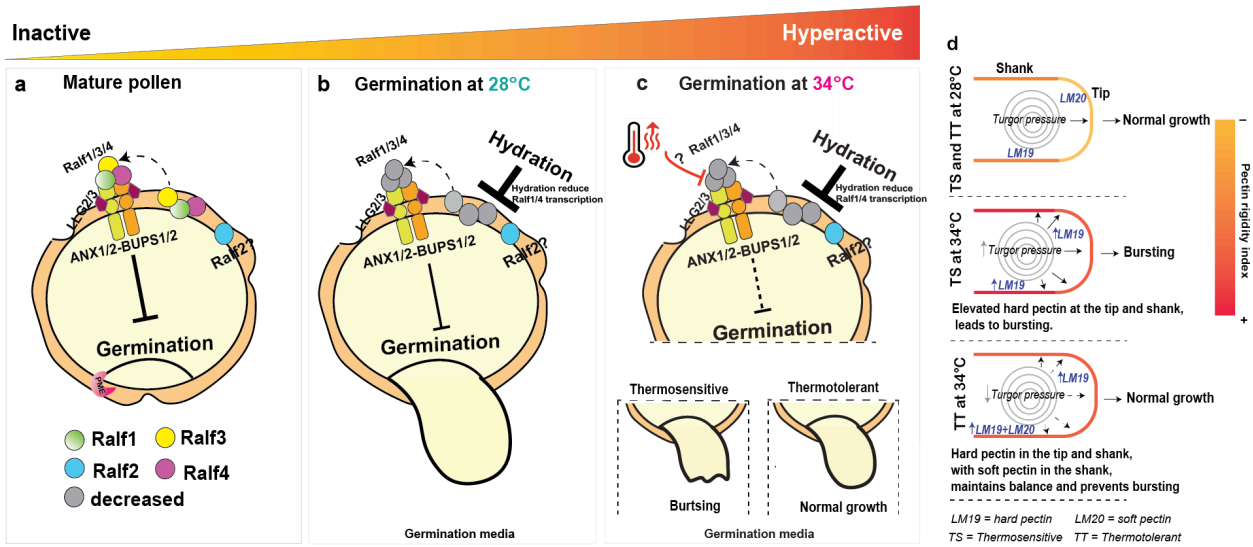

Figure 7. RALF signaling controls thermotolerant pollen tube growth. (a) In mature pollen, high levels of RALF1, RALF3, and RALF4 bind to their receptors ANX1/2 and BUPS1/2 and the co-receptor LLG2/3, inhibiting pollen germination and maintaining pollen dormancy (Inactive). **(b)** Upon pollen hydration and the initiation of germination, levels of RALF1 and RALF4 decrease, reducing inhibition and allowing pollen tube extension. A tightly regulated balance of RALF peptides is crucial for proper germination. **(c)** Under high temperature (34°), RALF signaling is disrupted in thermosensitive genotypes, leading to hyperactivation and rupture. We propose that RALF signaling is maintained at HT in thermotolerant cultivars. **(d)** This differential thermoresponse is associated with variations in cell wall composition and pectin distribution between cultivars. The schematic illustrates dynamic changes in pectin distribution and rigidity at 28° and 34° in thermosensitive (TS) and thermotolerant (TT) cultivars. At 34°, rigid pectin (identified by LM19 antibody) in creases across the tube in thermosensitive cultivars, leading to bursting. In contrast, in thermotolerant cultivars, heat stress also elevates soft pectin (identified by LM20 antibody) in the shank, which may reduce wall rigidity to maintain pollen tube integrity. The color scale indicates the pectin rigidity index. Upward and downward arrows indicate observed increases and decreases, respectively.

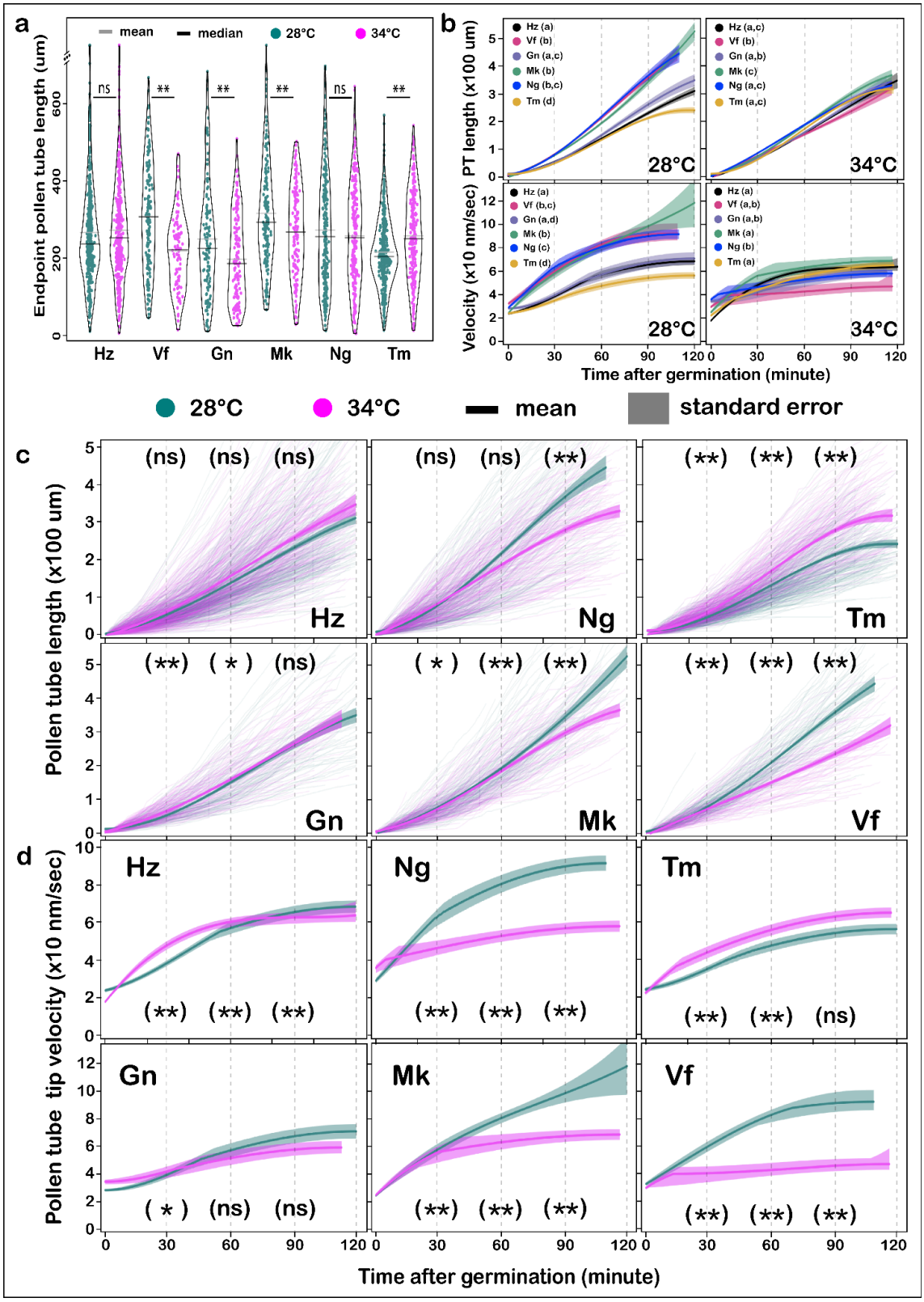
a
mean
median
28°C
34°C
Endpoint pollen tube length (um)
ns
**
Hz
Vf
Gn
Mk
Ng
Tm
b
PT length (x100 um)
Velocity (x10 nm/sec)
Hz (a)
Vf (b)
Gn (a,c)
Mk (b)
Ng (b,c)
Tm (d)
Hz (a,c)
Vf (b)
Gn (a,b)
Mk (c)
Ng (a,c)
Tm (a,c)
Hz (a)
Vf (b,c)
Gn (a,d)
Mk (b)
Ng (c)
Tm (d)
Hz (a)
Vf (a,b)
Gn (a,b)
Mk (a)
Ng (b)
Tm (a)
28°C
34°C
Time after germination (minute)
28°C
34°C
mean
standard error
c
Pollen tube length (x100 um)
(ns) (ns) (ns)
(ns) (ns) (**)
(**) (**) (**)
Hz
Ng
Tm
(**) (*) (ns)
(*) (**) (**)
(**) (**) (**)
Gn
Mk
Vf
d
Pollen tube tip velocity (x10 nm/sec)
Hz
Ng
Tm
(**) (**) (**)
(**) (**) (**)
(**) (**) (ns)
Gn
Mk
Vf
(*) (ns) (ns)
(**) (**) (**)
(**) (**) (**)
Time after germination (minute)

Supplemental Figure 1: Related to Figure 1. Effects of high temperature on pollen tube elongation and tip velocity. (a) PT length at 120 minutes without taking into account time of germination. Statistical analysis determined using the Welch Two Sample t-test with p.value ranges of ns>0.05>*>*0.01*>**. **(b)** Comparison of the evolution of pollen tube length across all genotypes analyzed. Statistical significance was determined using the Welch Two Sample t-test at 90 minutes of growth. Shared letters indicate no statistical significance at $p < 0.01$. **(c)** Comparison of velocity across all genotypes analyzed. Statistical significance was determined using Dunn's test. Shared letters indicate no statistical significance at $p < 0.01$. **(d)** Effects of temperature on pollen tube length over time. Statistical analysis was done at 30 minutes, 60 minutes, and 90 minutes after germination using the Welch Two Sample t-test using p.value ranges of ns>0.05>*>*0.01*>**. **(e)** Effects of temperature on pollen tube velocity. Statistical analysis was performed as described in (d) but using the Mann-Whitney-Wilcoxon U test.

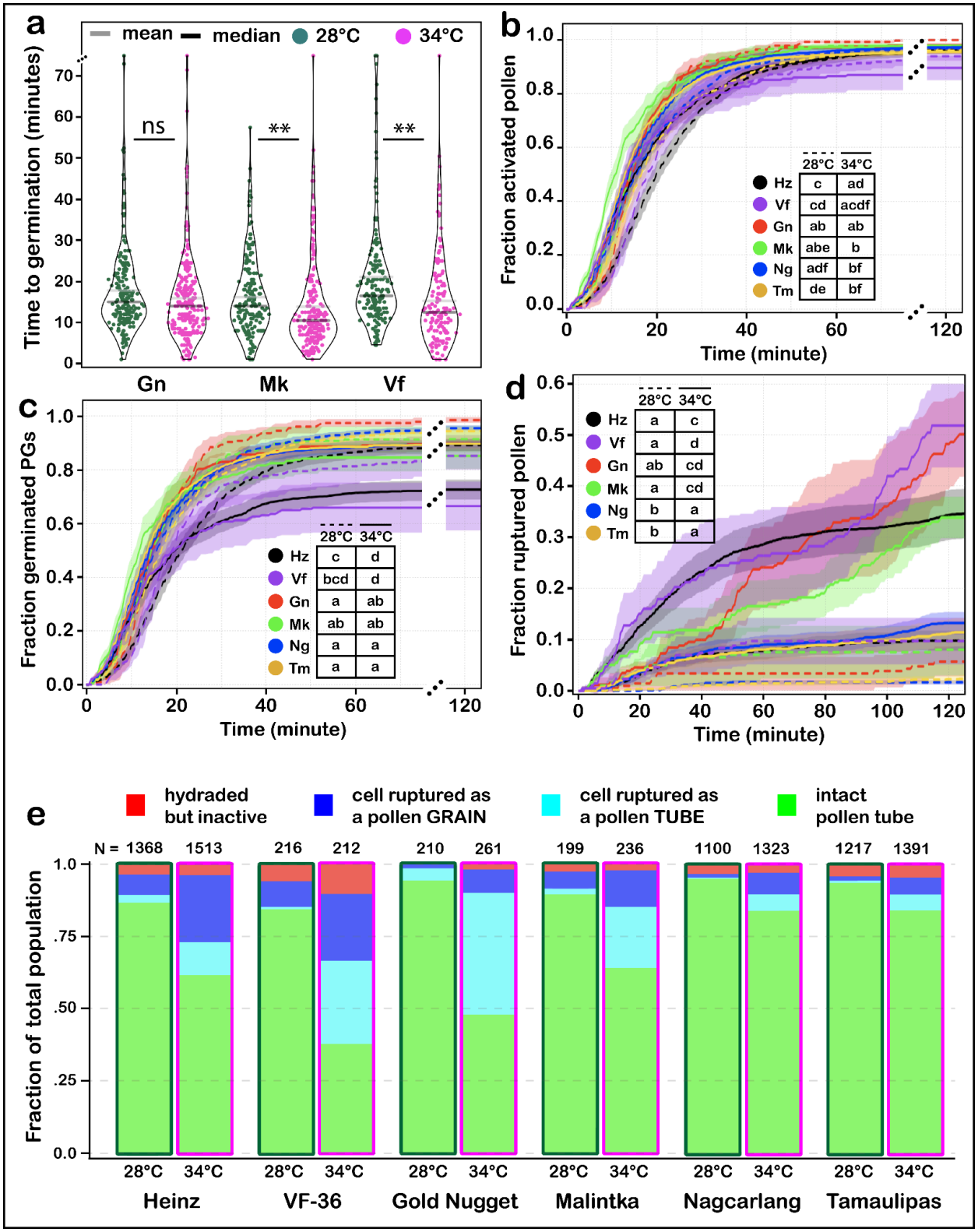

Supplemental Figure 2: Related to Figure 1. Effects of High temperature on pollen performance. (a) Time to successful germination at indicated temperatures for gold nugget

(Gn), Malintka (Mk), and VF-36 (Vf). Each dot represents a germinated pollen grain. Statistical analysis was performed using the Mann-Whitney-Wilcoxon U test using p.value thresholds of ns > 0.01 > * > 0.001 > **. **(b)** Fraction of activated pollen grains over time. **(c)** Fraction of successfully germinated pollen grains over time. **(d)** Fraction of ruptured pollen grains and tubes over time. For **a-d,** Statistical analysis was performed using survival analysis (methods) with a time cutoff of 120 minutes and pairwise p.values were bonferroni adjusted. Similar letters in tables represent no statistical significance between groups at a p.value < 0.01. Different letters in tables represent statistically significant differences at a p.value < 0.01 between groups. **(e)** Cumulative barplots showing the density of each pollen performance population tracked.

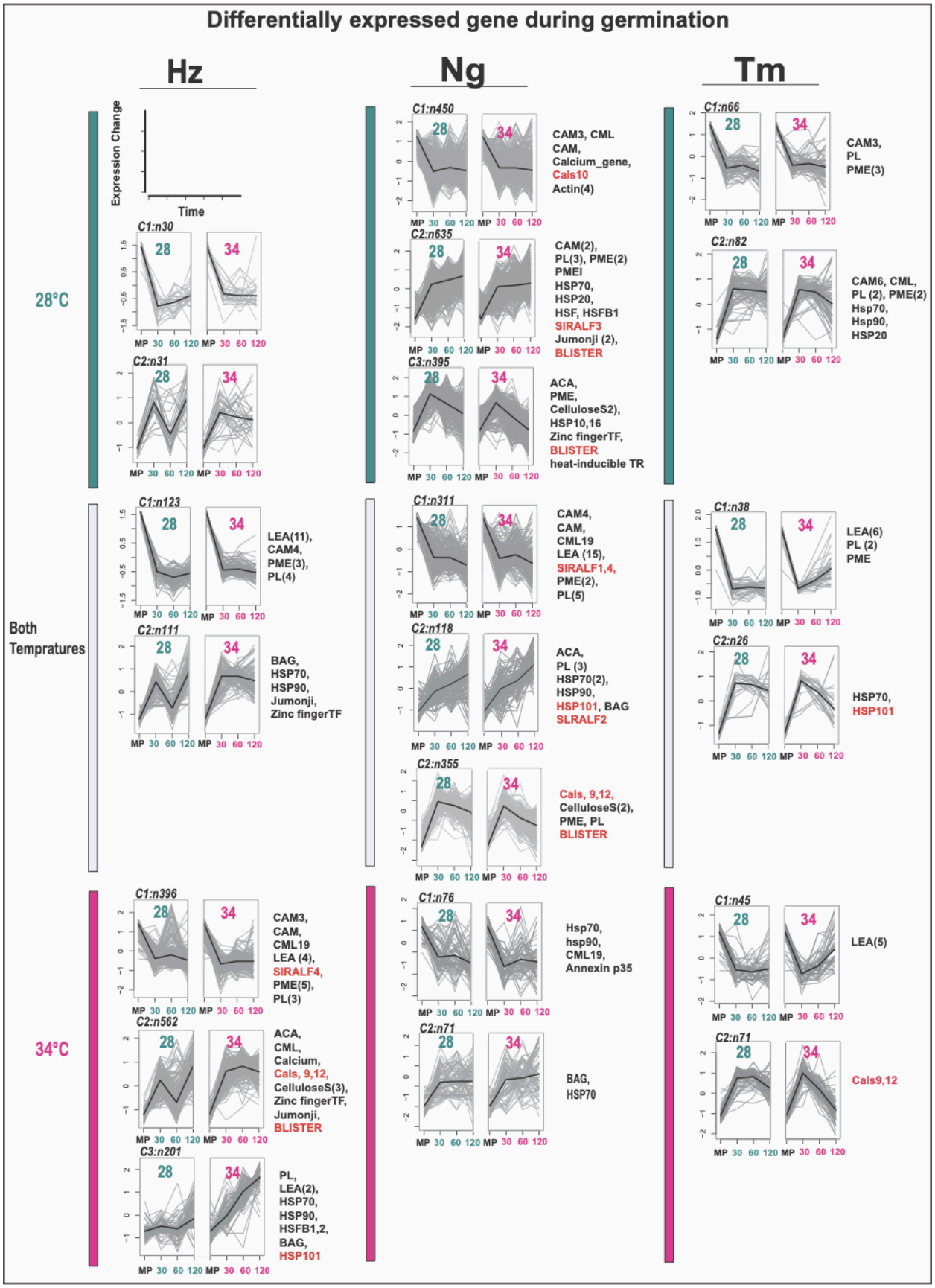
Differentially expressed gene during germination
Hz
Ng
Tm
Expression Change
Time
28°C
Both Tempratures
34°C
C1:n30
C2:n31
C1:n123
C2:n111
C1:n396
C2:n562
C3:n201
C1:n450
C2:n635
C3:n395
C1:n311
C2:n118
C2:n355
C1:n76
C2:n71
C1:n66
C2:n82
C1:n38
C2:n26
C1:n45
C2:n71
28
34
MP 30 60 120
LEA(11), CAM4, PME(3), PL(4)
BAG, HSP70, HSP90, Jumonji, Zinc fingerTF
CAM3, CAM, CML19 LEA (4), SIRALF4, PME(5), PL(3)
ACA, CML, Calcium, Cals, 9,12, CelluloseS(3), Zinc fingerTF, Jumonji, BLISTER
PL, LEA(2), HSP70, HSP90, HSFB1,2, BAG, HSP101
CAM3, CML CAM, Calcium_gene, Cals10 Actin(4)
CAM(2), PL(3), PME(2) PMEI HSP70, HSP20, HSF, HSFB1 SIRALF3 Jumonji (2), BLISTER
ACA, PME, CelluloseS2), HSP10,16 Zinc fingerTF, BLISTER heat-inducible TR
CAM4, CAM, CML19 LEA (15), SIRALF1,4, PME(2), PL(5)
ACA, PL (3) HSP70(2), HSP90, HSP101, BAG SLRALF2
Cals, 9,12, CelluloseS(2), PME, PL BLISTER
Hsp70, hsp90, CML19, Annexin p35
BAG, HSP70
CAM3, PL PME(3)
CAM6, CML, PL (2), PME(2) Hsp70, Hsp90, HSP20
LEA(6) PL (2) PME
HSP70, HSP101
LEA(5)
Cals9,12

Supplemental Figure 3: Related to Figure 2. transcriptomic profile analysis of pollen germination in different tomato cultivars. Clustering analysis of DEGs identified in Figure 3, Panel C, representing the transcriptomic changes during pollen germination in various tomato cultivars. Each cluster reflects a distinct pattern of protein expression across the different varieties.

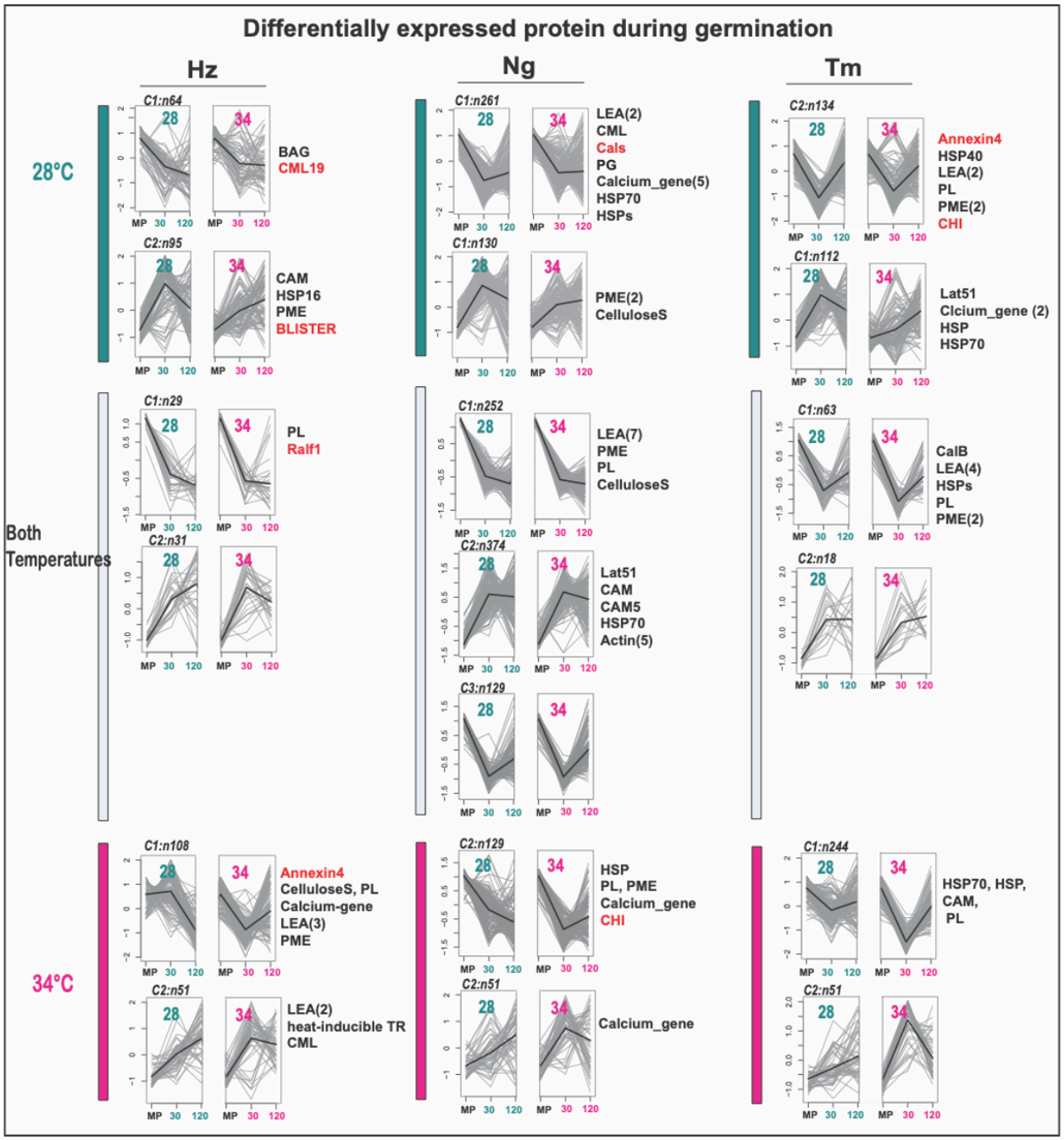

Supplemental Figure 4: Related to Figure 2. Proteomic profile Analysis of pollen germination in different tomato cultivars. Clustering analysis of DEPs identified in Figure 3, Panel C, representing the proteomic changes during pollen germination in various tomato cultivars. Each cluster reflects a distinct pattern of protein expression across the different varieties.

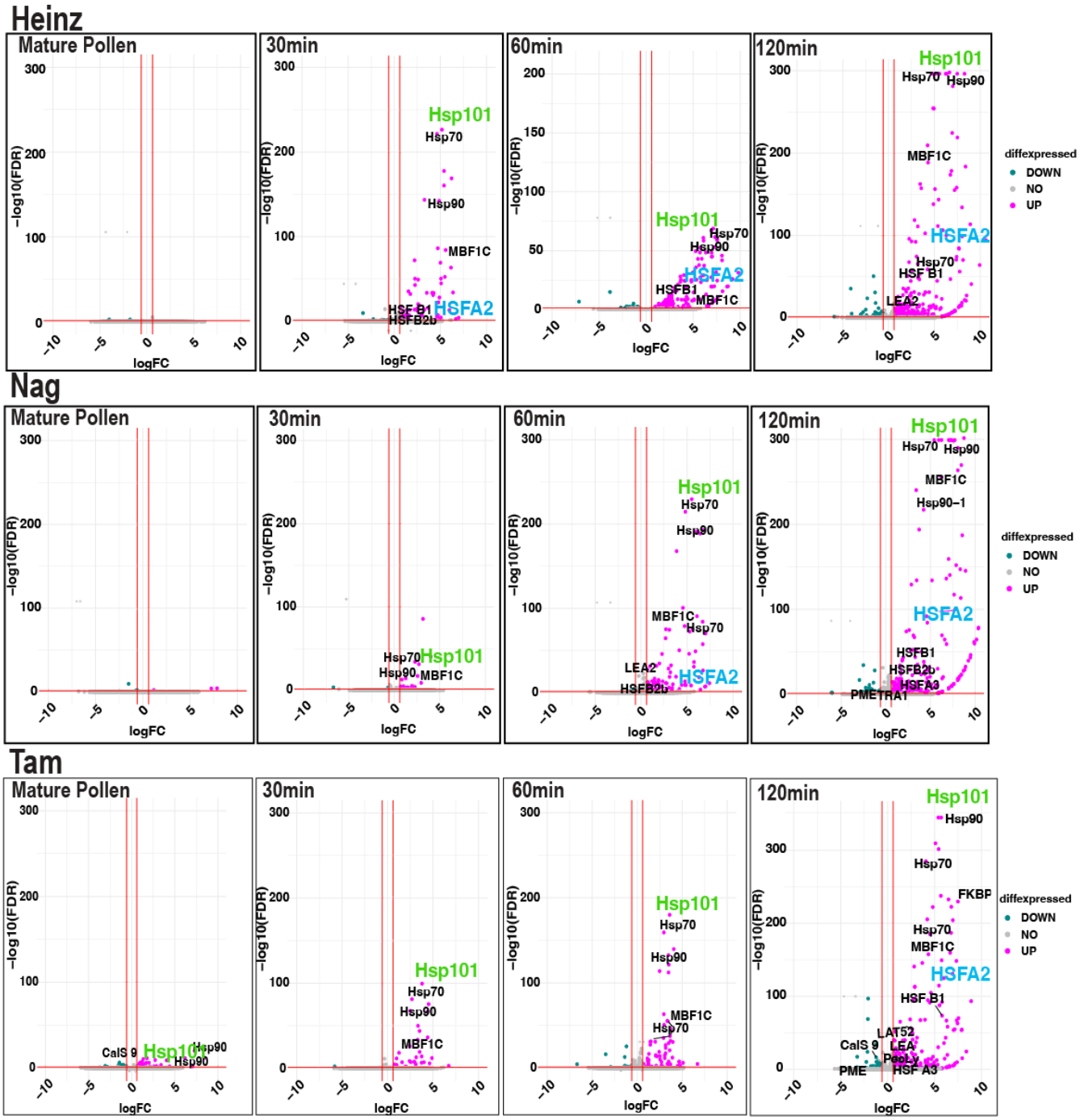

Supplementary Figure 5: Related to Figure 2. Volcano plot showing DEGs between 28° and 34° across cultivars at different time points. Genes with an absolute log fold change ≥ 0.5 and an adjusted p-value < 0.05 were considered significantly differentially expressed. Upregulated genes (logFC ≥ +0.5) are highlighted in magenta, and downregulated genes (logFC ≤ –0.5) are

shown in cyan. Selected heat stress–related genes, including HSP101, HSP90, HSP70, HSFA2, HSFB1, and MBF1C are highlighted in the plot to indicate their dynamic expression in response to heat conditions.

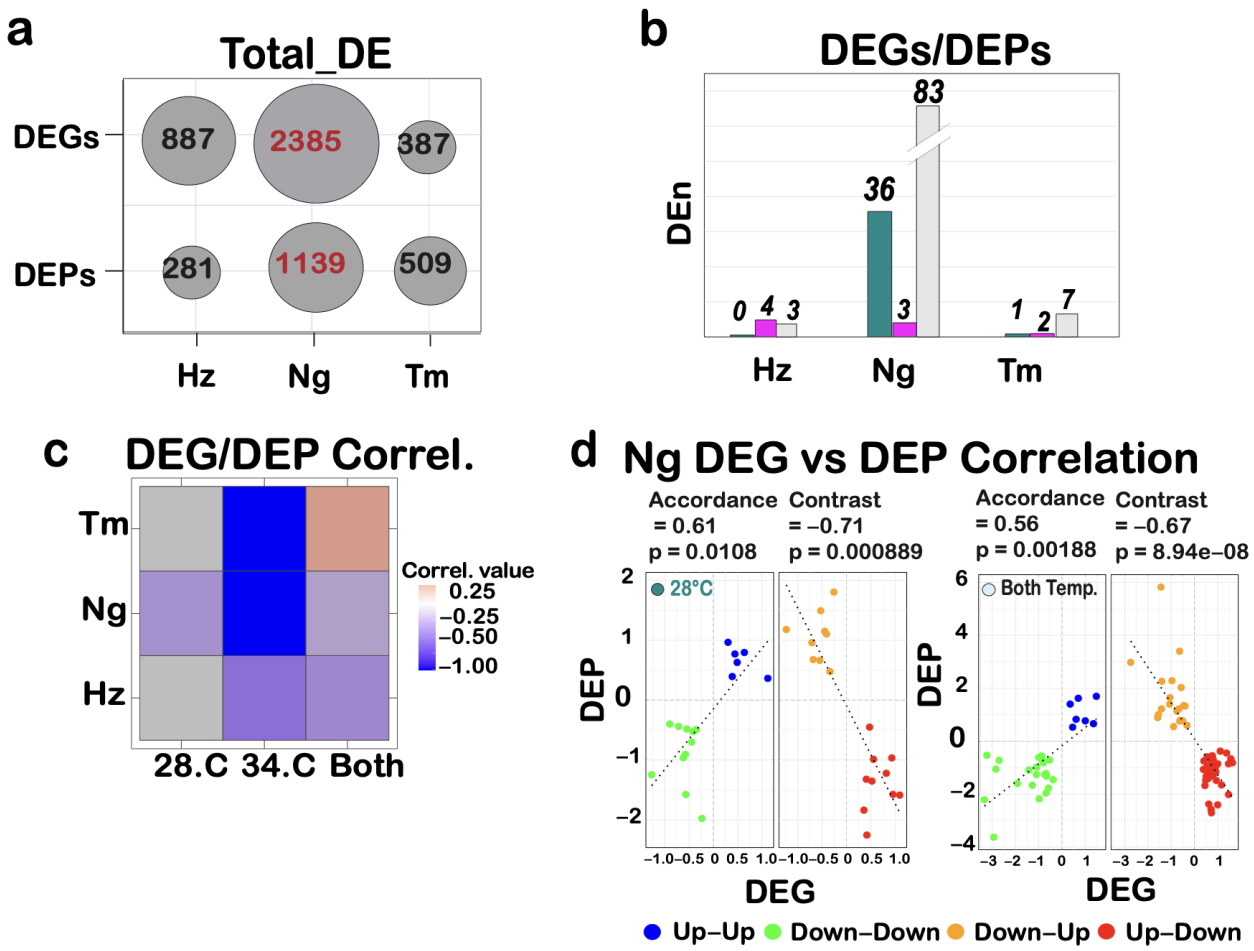

Supplemental Figure 6: Related to Figure 2. Negative Correlation Between Transcript and Protein Levels. (c) Heat map showing the correlation between DEPs and DEGs across three tomato cultivars under 28°, 34°, and both temperature conditions. Color intensity represents the Spearman correlation coefficient between transcriptomic and proteomic changes. A value of –1 indicates a strong negative correlation, while gray reflects insufficient overlap or undetectable correlation due to limited shared genes or proteins. (d) Transcript-protein correlation among shared DEGs and DEPs in Nagcarlang at 28° (n = 36) and both temperature conditions (n = 83).

Each point represents a gene-protein pair, colored by the direction of transcript and protein regulation: Up-Up (blue), Down-Down (green), Up-Down (red), and Down-Up (orange). Genes with concordant expression (Up-Up and Down-Down) showed a moderate positive Spearman correlation ($\rho = 0.56$, $p = 0.0018$), while those with opposing regulation (Up-Down and Down-Up) exhibited a strong negative correlation ($\rho = -0.71$, $p = 0.0001$).

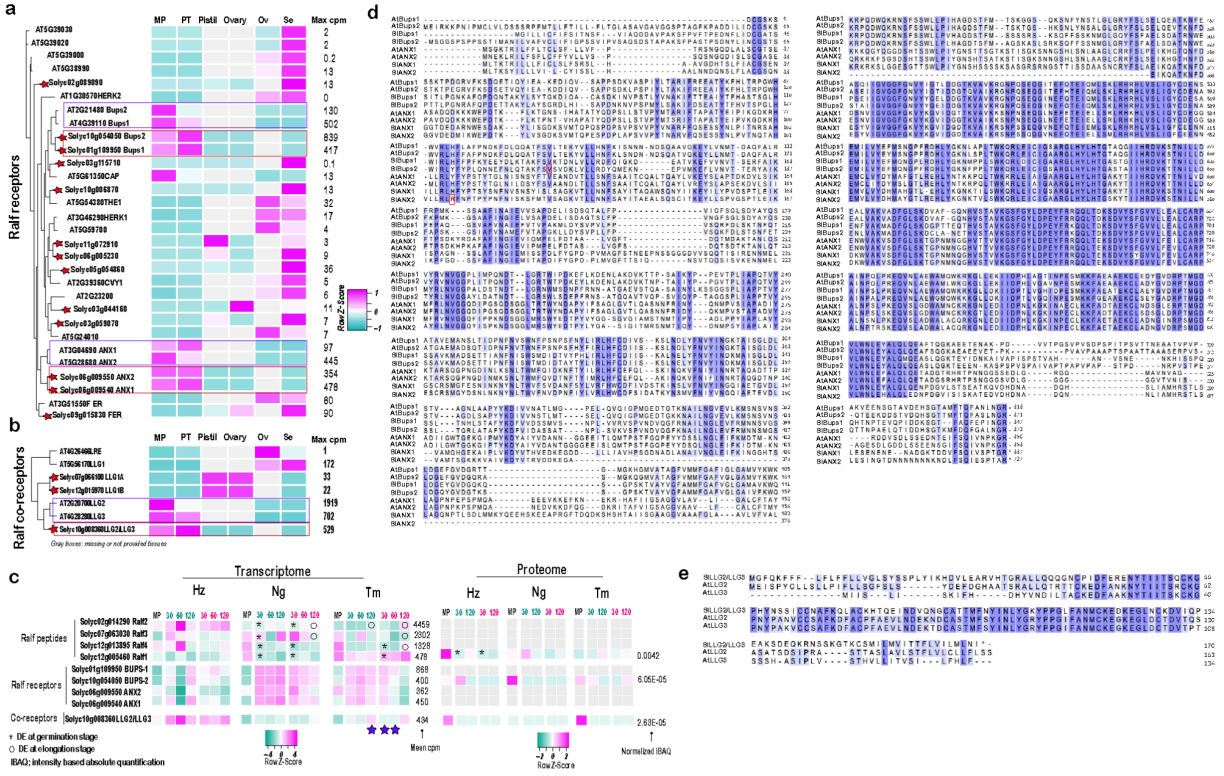

Supplemental Figure 7 : Related to Figure 3. Tomato pollen expresses four RALF receptors and two co-receptors. Phylogenetic tree illustrates the evolutionary relationships between tomato and Arabidopsis Ralf receptors **(a)** and Co-receptors **(b)**. Additionally, a heatmap shows the expression levels (RNA) of these genes in different tissues such as mature pollen "MP", pollen tube "PT", pistil, ovary, ovule "Ov" and seedling "Se". Max cpm represents the highest expression value observed across the different tissues. Gray boxes in the heatmap indicate tissues for which data are missing or not provided. **(d, e)** Multiple sequence alignments

of the most abundantly expressed RALF receptors (c) and co-receptors (d) in mature pollen and the pollen tube, compared with their Arabidopsis homologs. Conserved amino acid residues are shaded. In panel (c), red boxes highlight genotype-specific amino acid variations observed in the Nagcarlang: arginine (R) residue in SlANX2 and a valine (V) in SlBUPS2 in the Hz correspond to a histidine (H) and an alanine (A), respectively, in the Ng cultivar.

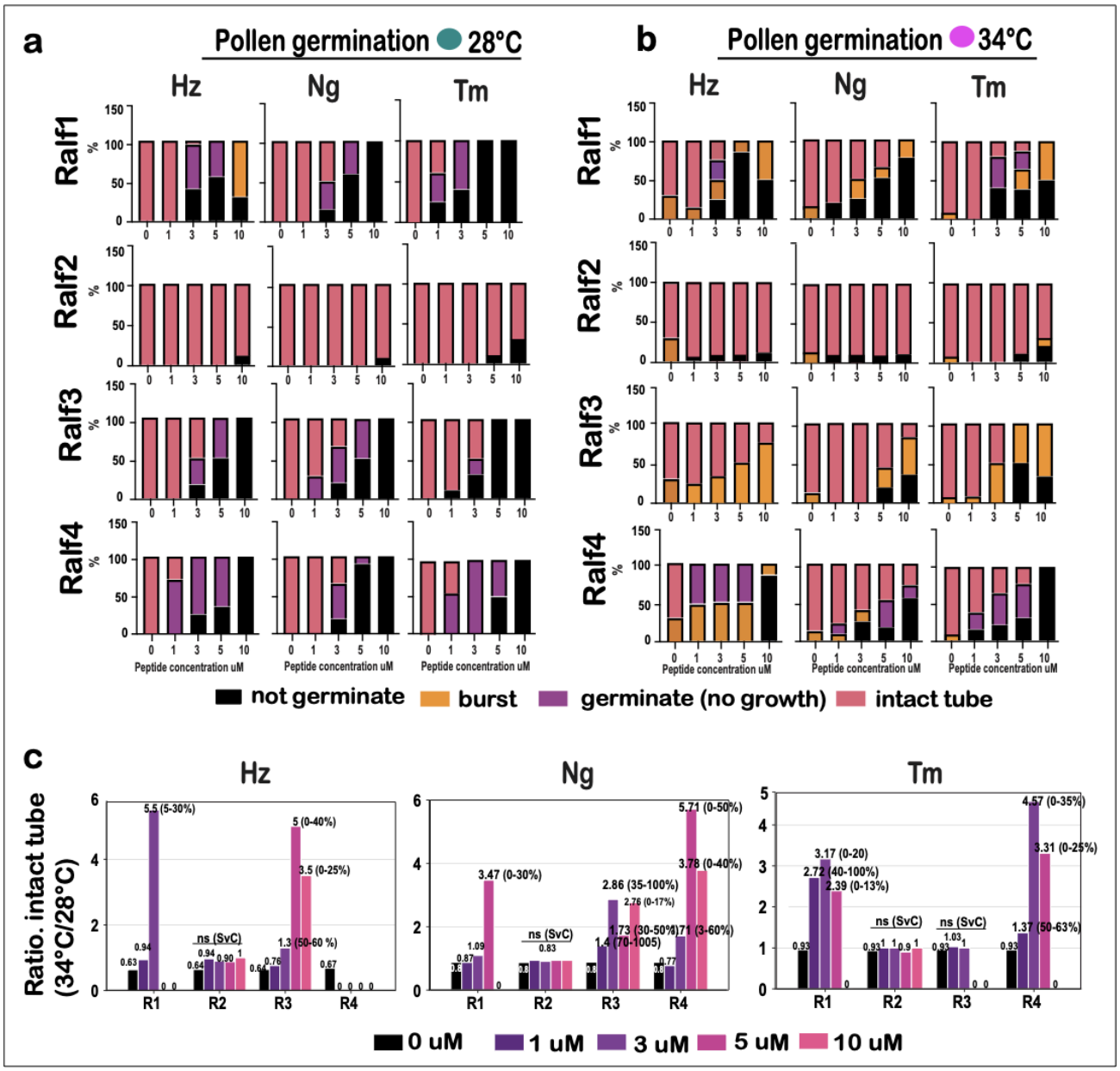

Supplemental Figure 8: Related to Figure 4. Effects of different RALF peptides on pollen tube germination under **(a)** 28° or 34°**. (c)** Ratio of percentage of pollen tube formation between control and heat stress, a ratio greater than 1 indicates an enhancement of pollen tube formation under heat stress compared to control (%) represents the increase of pollen tube formation by HT. We grew Heinz, Nagcarlang, and Tamaulipas pollen with each peptide at 1, 3, 5, and 10 μM for 90 minutes at 28° and evaluated pollen germination and tube elongation. 10 uM SlRALF4 and SlRALF3 completely inhibited pollen germination of all three cultivars, whereas 10 uM SlRALF1 inhibited germination in Nagcarlang and Tamaulipas, but caused ~80% of pollen to rupture in Heinz. SlRALF1, 3, and 4 all showed dose-dependent inhibition of pollen germination between concentrations of 1 and 10 uM that varied across the three cultivars. SlRALF2 had little effect on pollen germination even at 10 uM. These data suggest that SlRALFs 1, 3, and 4, but not SlRALF2 control pollen germination and that responses vary across cultivars. These findings are consistent with previous analysis of SlRALF3 (SlPRALF[22]). To test whether RALF signaling interacts with temperature, we conducted these experiments at HT (34°). Unlike our observations at 28°, 10 uM SlRALF3 did not completely inhibit pollen germination of any of the cultivars at 34°. Instead, at HT significant numbers of pollen burst (Heinz, Nagcarlang, and Tamaulipas) or produced an intact PT (Heinz and Nagcarlang). The germination-blocking effects of SlRALF1 and SlRALF4 were also partially reversed at 34°. Again, SlRALF2 treatment had little effect on PT growth at 34°. These data suggest that HT is antagonistic to RALF (SlRALF1, 3, and 4) signaling.

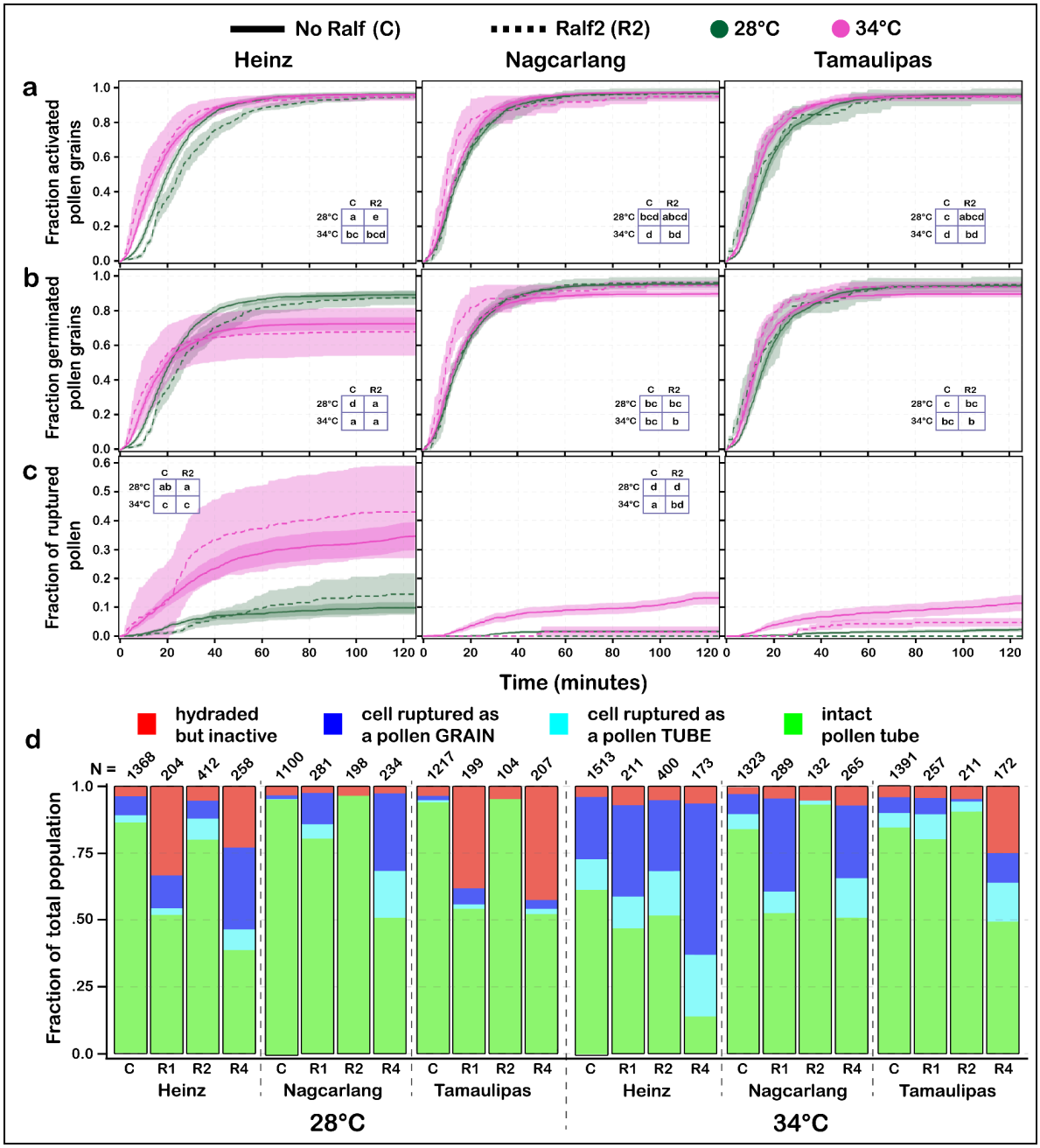

Supplemental Figure 9: Related to Figure 4. Effects of SlRalf2 on pollen grain activation, germination, and cell rupture. (a) Fraction of activated pollen grains over time – grains that exited the hydrated state (Figure 1a, red). **(b)** Fraction of successfully germinated pollen grains over time (Figure 1a, red to green). **(c)** Fraction of ruptured pollen grains and tubes over time (Figure 1a, blue + cyan). For c-e, Statistical analysis was performed using survival analysis (methods) with a time cutoff of 125 minutes and pairwise p.values were bonferroni adjusted.

Similar letters in tables represent no statistical significance between groups at a p.value < 0.01. Different letters in tables represent statistically significant differences at a p.value < 0.01 between groups. **(d)** Cumulative barplots showing the density of each pollen performance population tracked.

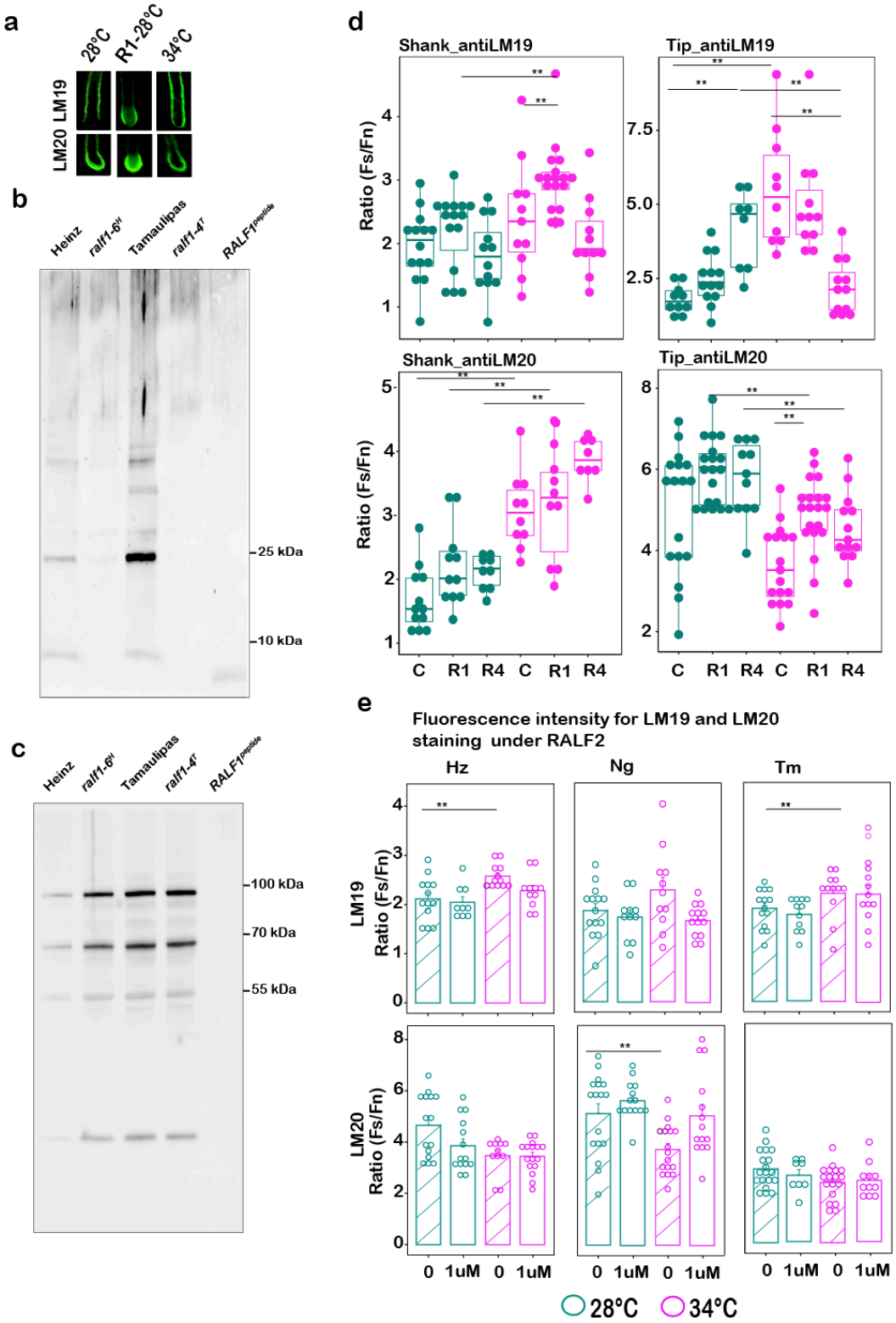
a
28°C
R1-28°C
34°C
LM19
LM20
b
Heinz
ralf1-6
Tamaulipas
ralf1-4
RALF1peptide
25 kDa
10 kDa
c
Heinz
ralf1-6
Tamaulipas
ralf1-4
RALF1peptide
100 kDa
70 kDa
55 kDa
d
Shank_antiLM19
Tip_antiLM19
Shank_antiLM20
Tip_antiLM20
Ratio (Fs/Fn)
C R1 R4 C R1 R4
e
Fluorescence intensity for LM19 and LM20 staining under RALF2
Hz
Ng
Tm
LM19 Ratio (Fs/Fn)
LM20 Ratio (Fs/Fn)
0 1uM 0 1uM
28°C
34°C

Supplemental Figure 10, related to Figure 6: (a) Representative images of LM19 and LM20 immunostaining, showing pectin distribution in the shank and tip regions of pollen tubes in Nagcarlang. RALF1 (R1) treatment is used as a representative for staining patterns. **(b, c)** Complete Western blot analysis using anti-RALF1 and anti-PEPC antibodies, respectively, in WT Heinz, WT Tamaulipas, mutant lines, and synthetic RALF1 peptide. **(d)** Quantification of fluorescence intensity for LM19 and LM20 staining in the shank and tip region under RALF1 and RALF4 treatments in Nagcarlang , and at 23° and 34°. Fluorescence intensity was normalized using the ratio of LM19 or LM20-stained fluorescence (Fs) to fluorescence of unstained controls (Fn). Statistical significance was determined using Dunn test and indicated as $p < 0.01$ (**), only . **(e**) Quantification of fluorescence intensity for LM19 staining in the shank region and LM20 staining in the tip under RALF2 treatment across cultivars at 23° and 34°. Fluorescence intensity was normalized using the ratio of LM19- or LM20-stained fluorescence (Fs) to the fluorescence of unstained controls (Fn). Statistical significance was determined using the Dunn test and indicated as **$p < 0.01$. Only significant values are shown in the graph (indicated by two asterisks).

References

1. Wheeler, T. R., Craufurd, P. Q., Ellis, R. H., Porter, J. R. & Vara Prasad, P. V. Temperature variability and the yield of annual crops. *Agric. Ecosyst. Environ.* **82**, 159–167 (2000).
2. Brown, S. J. Future changes in heatwave severity, duration and frequency due to climate change for the most populous cities. *Weather and Climate Extremes* **30**, 100278 (2020).
3. Brown, P. T. & Caldeira, K. Greater future global warming inferred from Earth's recent energy budget. *Nature* **552**, 45–50 (2017).
4. Battisti, D. S. & Naylor, R. L. Historical warnings of future food insecurity with unprecedented seasonal heat. *Science* **323**, 240–244 (2009).
5. Peet, M. M., Sato, S. & Gardner, R. G. Comparing heat stress effects on male-fertile and male-sterile tomatoes. *Plant Cell Environ.* **21**, 225–231 (1998).
6. Sato, S., Peet, M. M. & Thomas, J. F. Physiological factors limit fruit set of tomato (Lycopersicon esculentum Mill.) under chronic, mild heat stress. *Plant Cell Environ.* **23**, 719–726 (2000).
7. Sato, S., Peet, M. M. & Thomas, J. F. Determining critical pre- and post-anthesis periods and physiological processes in Lycopersicon esculentum Mill. exposed to moderately elevated temperatures. *J. Exp. Bot.* **53**, 1187–1195 (2002).
8. Abiko, M. *et al.* High-temperature induction of male sterility during barley (Hordeum vulgare L.) anther development is mediated by transcriptional inhibition. *Sex. Plant Reprod.* **18**, 91–100 (2005).
9. Sato, S. *et al.* Moderate increase of mean daily temperature adversely affects fruit set of Lycopersicon esculentum by disrupting specific physiological processes in male reproductive development. *Ann. Bot.* **97**, 731–738 (2006).
10. Oshino, T. *et al.* Premature progression of anther early developmental programs accompanied by comprehensive alterations in transcription during high-temperature injury

in barley plants. *Mol. Genet. Genomics* **278**, 31–42 (2007).

11. Endo, M. *et al.* High temperatures cause male sterility in rice plants with transcriptional alterations during pollen development. *Plant Cell Physiol.* **50**, 1911–1922 (2009).
12. Fragkostefanakis, S. *et al.* HsfA2 Controls the Activity of Developmentally and Stress-Regulated Heat Stress Protection Mechanisms in Tomato Male Reproductive Tissues. *Plant Physiol.* **170**, 2461–2477 (2016).
13. Ferris, R., Ellis, R. H., Wheeler, T. R. & Hadley, P. Effect of High Temperature Stress at Anthesis on Grain Yield and Biomass of Field-grown Crops of Wheat. *Ann. Bot.* **82**, 631–639 (1998).
14. Zinn, K. E., Tunc-Ozdemir, M. & Harper, J. F. Temperature stress and plant sexual reproduction: uncovering the weakest links. *J. Exp. Bot.* **61**, 1959–1968 (2010).
15. Johnson, M. A., Harper, J. F. & Palanivelu, R. A Fruitful Journey: Pollen Tube Navigation from Germination to Fertilization. *Annu. Rev. Plant Biol.* **70**, 809–837 (2019).
16. Okuda, S. *et al.* Defensin-like polypeptide LUREs are pollen tube attractants secreted from synergid cells. *Nature* **458**, 357–361 (2009).
17. Márton, M. L., Cordts, S., Broadhvest, J. & Dresselhaus, T. Micropylar pollen tube guidance by egg apparatus 1 of maize. *Science* **307**, 573–576 (2005).
18. Hamamura, Y. *et al.* Live-cell imaging reveals the dynamics of two sperm cells during double fertilization in Arabidopsis thaliana. *Curr. Biol.* **21**, 497–502 (2011).
19. Ouonkap, S. V. Y. *et al.* Enhanced pollen tube performance at high temperature contributes to thermotolerant fruit and seed production in tomato. *Curr. Biol.* **34**, 5319–5333.e5 (2024).
20. Boisson-Dernier, A. *et al.* ANXUR receptor-like kinases coordinate cell wall integrity with growth at the pollen tube tip via NADPH oxidases. *PLoS Biol.* **11**, e1001719 (2013).
21. Pearce, G., Moura, D. S., Stratmann, J. & Ryan, C. A., Jr. RALF, a 5-kDa ubiquitous polypeptide in plants, arrests root growth and development. *Proc. Natl. Acad. Sci. U. S. A.* **98**, 12843–12847 (2001).

22. Covey, P. A. *et al.* A pollen-specific RALF from tomato that regulates pollen tube elongation. *Plant Physiol.* **153**, 703–715 (2010).
23. Ge, Z. *et al.* Arabidopsis pollen tube integrity and sperm release are regulated by RALF-mediated signaling. *Science* **358**, 1596–1600 (2017).
24. Mecchia, M. A. *et al.* RALF4/19 peptides interact with LRX proteins to control pollen tube growth in Arabidopsis. *Science* **358**, 1600–1603 (2017).
25. Ge, Z. *et al.* LLG2/3 Are Co-receptors in BUPS/ANX-RALF Signaling to Regulate Arabidopsis Pollen Tube Integrity. *Curr. Biol.* **29**, 3256–3265.e5 (2019).
26. Zhou, X. *et al.* Membrane receptor-mediated mechano-transduction maintains cell integrity during pollen tube growth within the pistil. *Dev. Cell* **56**, 1030–1042.e6 (2021).
27. Moussu, S. *et al.* Plant cell wall patterning and expansion mediated by protein-peptide-polysaccharide interaction. *Science* **382**, 719–725 (2023).
28. Moussu, S. *et al.* Structural basis for recognition of RALF peptides by LRX proteins during pollen tube growth. *Proc. Natl. Acad. Sci. U. S. A.* **117**, 7494–7503 (2020).
29. Fabrice, T. N. *et al.* LRX Proteins Play a Crucial Role in Pollen Grain and Pollen Tube Cell Wall Development. *Plant Physiol.* **176**, 1981–1992 (2018).
30. Zhou, L.-Z. *et al.* The RALF signaling pathway regulates cell wall integrity during pollen tube growth in maize. *Plant Cell* **36**, 1673–1696 (2024).
31. Ouonkap, S. V. Y., Oseguera, Y., Okihiro, B. & Johnson, M. A. Semi-automated high content analysis of pollen performance using tubetracker. *Plant Reprod.* **38**, 16 (2025).
32. Abarca, A., Franck, C. M. & Zipfel, C. Family-wide evaluation of RAPID ALKALINIZATION FACTOR peptides. *Plant Physiol.* **187**, 996–1010 (2021).
33. Xiao, Y. *et al.* Mechanisms of RALF peptide perception by a heterotypic receptor complex. *Nature* **572**, 270–274 (2019).
34. Somoza, S. C. *et al.* Arabidopsis RALF4 rapidly halts pollen tube growth by increasing ROS and decreasing calcium cytoplasmic tip levels. *Biomolecules* **14**, 1375 (2024).

35. Schoenaers, S. *et al.* Rapid alkalinization factor 22 has a structural and signalling role in root hair cell wall assembly. *Nat. Plants* **10**, 494–511 (2024).
36. Verhertbruggen, Y., Marcus, S. E., Haeger, A., Ordaz-Ortiz, J. J. & Knox, J. P. An extended set of monoclonal antibodies to pectic homogalacturonan. *Carbohydr. Res.* **344**, 1858–1862 (2009).
37. Chebli, Y., Kaneda, M., Zerzour, R. & Geitmann, A. The Cell Wall of the Arabidopsis Pollen Tube—Spatial Distribution, Recycling, and Network Formation of Polysaccharides. *Plant Physiol.* **160**, 1940–1955 (2012).
38. Dardelle, F. *et al.* Biochemical and immunocytological characterizations of Arabidopsis pollen tube cell wall. *Plant Physiol.* **153**, 1563–1576 (2010).
39. Bosch, M. & Hepler, P. K. Pectin methylesterases and pectin dynamics in pollen tubes. *Plant Cell* **17**, 3219–3226 (2005).
40. Sze, H. *et al.* A wave of specific transcript and protein accumulation accompanies pollen dehydration. *Plant Physiol.* **195**, 1775–1795 (2024).
41. Sze, H., Palanivelu, R., Harper, J. F. & Johnson, M. A. Holistic insights from pollen omics: co-opting stress-responsive genes and ER-mediated proteostasis for male fertility. *Plant Physiol.* **187**, 2361–2380 (2021).
42. Zhong, S. *et al.* RALF peptide signaling controls the polytubey block in Arabidopsis. *Science* **375**, 290–296 (2022).
43. Noble, J. A. *et al.* Evolutionary analysis of the LORELEI gene family in plants reveals regulatory subfunctionalization. *Plant Physiol.* **190**, 2539–2556 (2022).
44. Parre, E. & Geitmann, A. Pectin and the role of the physical properties of the cell wall in pollen tube growth of Solanum chacoense. *Planta* **220**, 582–592 (2005).
45. Lehner, A. *et al.* Pectins in the cell wall of Arabidopsis thaliana pollen tube and pistil. *Plant Signal. Behav.* **5**, 1282–1285 (2010).
46. Perez-Riverol, Y. *et al.* The PRIDE database resources in 2022: a hub for mass

spectrometry-based proteomics evidences. *Nucleic Acids Res.* **50**, D543–D552 (2022).

47. Althiab-Almasaud, R. *et al.* Ethylene signaling modulates tomato pollen tube growth through modifications of cell wall remodeling and calcium gradient. *Plant J.* 1–16 (2021).
48. Towbin, H., Staehelin, T. & Gordon, J. Electrophoretic transfer of proteins from polyacrylamide gels to nitrocellulose sheets: procedure and some applications. *Proc. Natl. Acad. Sci. U. S. A.* **76**, 4350–4354 (1979).